# Coherence of light and matter: from basic concepts to modern applications

## Part III: G. Grübel

Script IV

### Coherence based X-ray techniques

Overview, Introduction to X-ray Scattering, Sources of Coherent X-rays, Speckle pattern and their analysis

### Imaging techniques

Phase Retrieval, Sampling Theory, Reconstruction of Oversampled Data, Fourier Transform Holography, Applications

### X-ray Photon Correlation Spectroscopy (XPCS)

Introduction, Equilibrium Dynamics (Brownian Motion), Surface Dynamics, Non-Equilibrium Dynamics

### Imaging and XPCS at FEL Sources

# Introduction: Scattering with coherent X-rays

If coherent light is scattered from a disordered system it gives rise to a random (grainy) diffraction pattern, known as "speckle". A speckle pattern is an interference pattern and related to the exact spatial arrangement of the scatterers in the disordered system.

$$I(Q,t) \sim S_c(Q,t) \sim | \sum e^{iQRj(t)} |^2$$

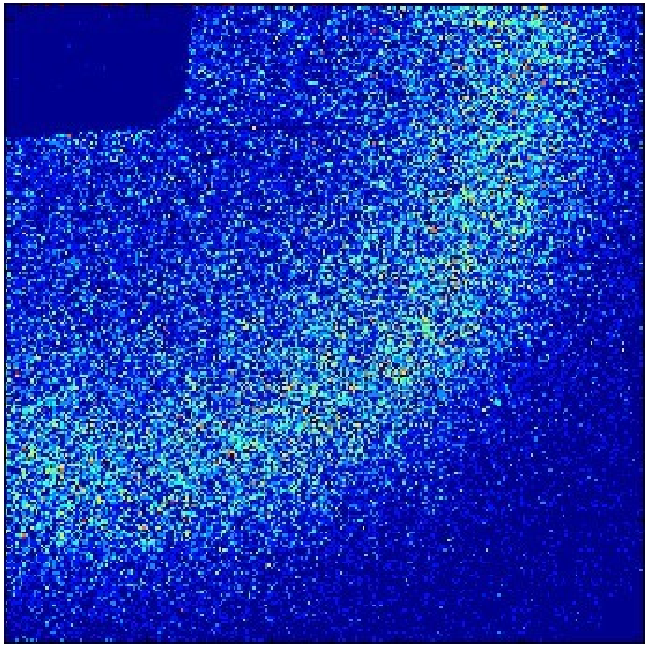

j in coherence volume $c = \xi_t^2 \xi_l$

Incoherent Light:

$S(Q,t) = \langle S_c(Q,t) \rangle_{V>>c}$ ensemble average

- quantify dynamics in terms of the intensity correlation function $g_2(Q,t)$:

$I(\mathbf{Q},t) = |\mathbf{E}(\mathbf{Q},t)|^2 = |\sum b_n(\mathbf{Q}) \exp[i\mathbf{Q}\bullet\mathbf{r}_n(t)|^2$

*Note:* $\mathbf{E}(\mathbf{Q},t) = \int d\mathbf{r}'\, \rho(\mathbf{r}') \exp[i\mathbf{Q}\bullet\mathbf{r}'(t)]$ $\rho(\mathbf{r}')$: *charge density*

$g_2(\mathbf{Q},t) = \langle I(\mathbf{Q},0) \bullet I(\mathbf{Q},t)\rangle / \langle I(\mathbf{Q})\rangle^2$

if $\mathbf{E}(\mathbf{Q},t)$ is a zero mean, complex gaussian variable:

$g_2(\mathbf{Q},t) = 1 + \beta(\mathbf{Q}) \langle \mathbf{E}(\mathbf{Q},0)\mathbf{E}^*(\mathbf{Q},t)\rangle^2 / \langle I(\mathbf{Q})\rangle^2$

$\langle\rangle$ ensemble av.; $\beta(\mathbf{Q})$ contrast

$g_2(\mathbf{Q},t) = 1 + \beta(\mathbf{Q}) |f(\mathbf{Q},t)|^2$ with $f(\mathbf{Q},t) = F(\mathbf{Q},t) / F(\mathbf{Q},0)$

$F(Q,0)$: static structure factor

N: number of scatterers

$F(\mathbf{Q},t) = [1/N\{b^2(\mathbf{Q})\} |\sum^N_{m=1}\sum^N_{n=1} \langle b_n(\mathbf{Q})b_m(\mathbf{Q})\bullet\exp\{i\mathbf{Q}[\mathbf{r}_n(0)-\mathbf{r}_m(t)]\}\rangle$

# A time correlation function $g_2(Q,\tau)$

$g_2(\mathbf{Q},t) = 1 + ß(\mathbf{Q})\, |f(\mathbf{Q},t)|^2$ and $f(Q,t) = \exp(-\Gamma\, t) = \exp(-t/\tau)$

β(Q)

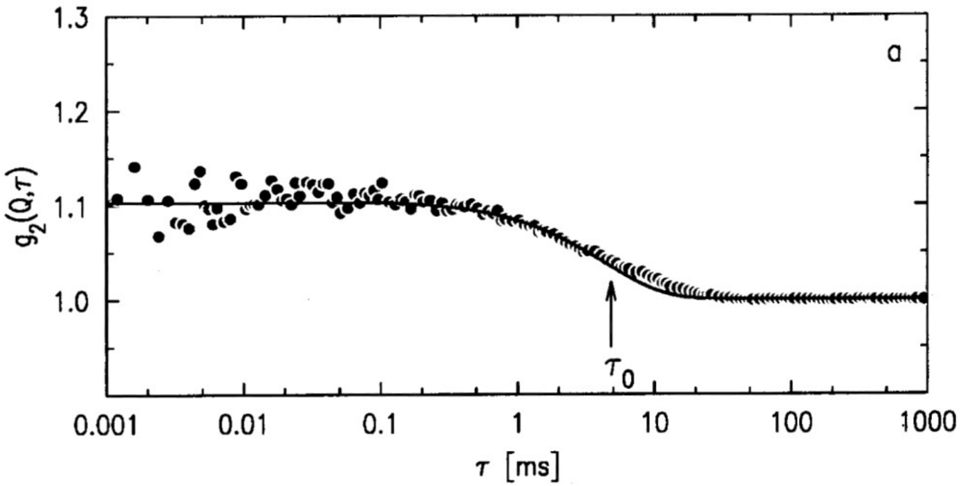


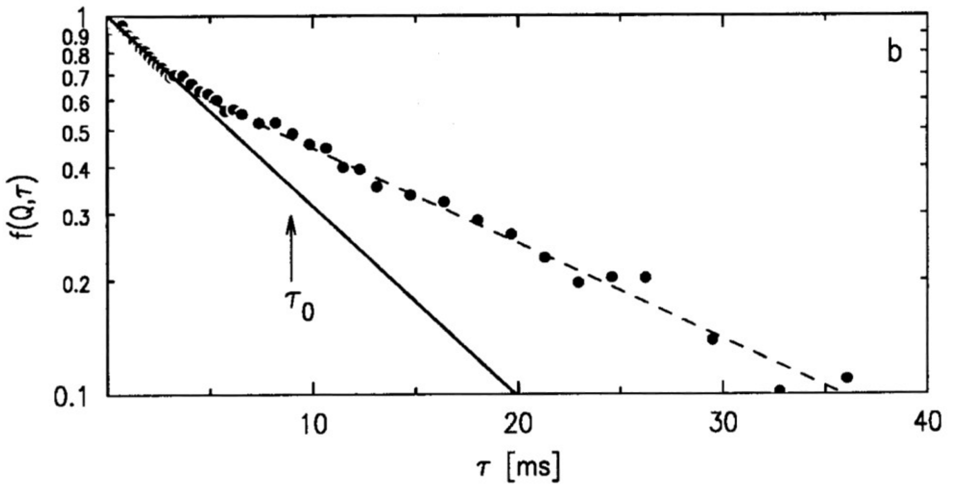

# Surface Sensitivity of X-Rays

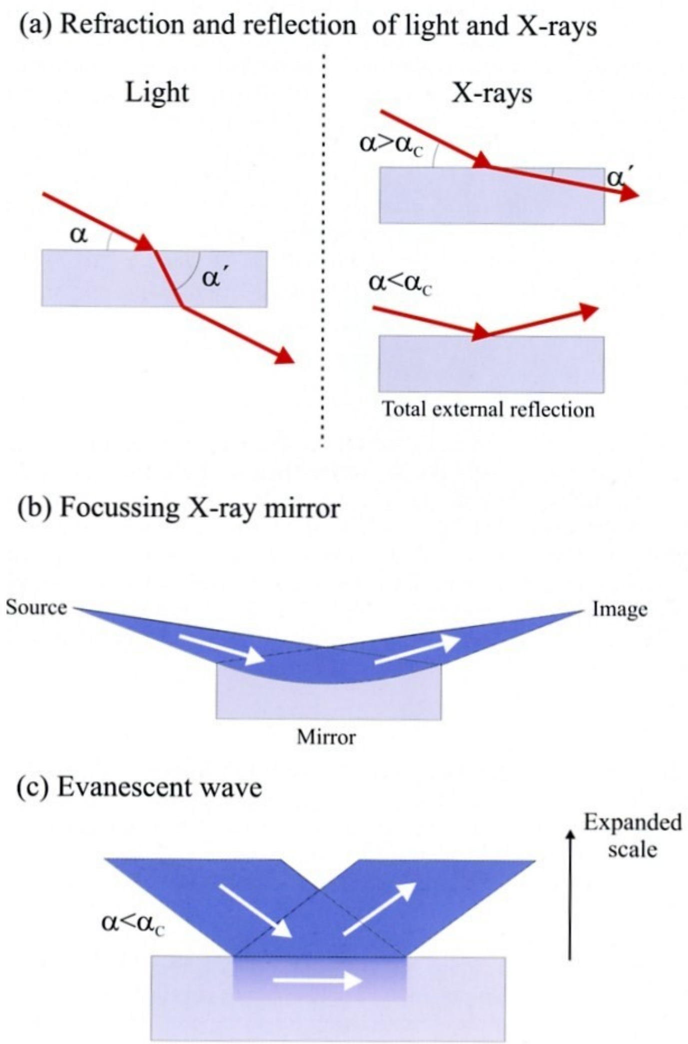


<u>refractive index:</u>

$n = 1 - \delta + i\,\beta$ = 1.5 - 1.8 visible light

<u>X-rays:</u> $\delta = 10^{-5}$ (solid matter)

$\beta \ll \delta$

$n < 1$

$\cos\alpha = n \bullet \cos\alpha'$

total external reflection for: $\alpha < \alpha_c$

for $\alpha' = 0$ (and $\beta$=0):

$\alpha_c = \sqrt{2\delta}$ [mrad]

$\alpha < \alpha_c$: evanescent wave with nanometer penetration

# Dynamics at Surfaces: Capillary Waves

Thermally excited capillary waves decorate the surfaces of all liquids depending on the surface tension $\sigma$ and the viscosity $\eta$.

Capillary wave:

$$\zeta(r,t) = \zeta_0 \exp(iq_{||}r - \omega t)$$

$$\omega = \omega_0 + i\Gamma$$

The linear Navier-Stokes equation for simple liquids yields:

**Low viscosity:** $\sigma\rho/4\eta^2 q_{||} > 1$

$\mathbf{\Gamma = (2\eta/\rho)\, q_{||}^2}$

$\mathbf{\omega_0 = \sqrt{(\sigma/\rho)}\, q_{||}^{3/2}}$

propagating wave

**High viscosity:** $\sigma\rho/4\eta^2 q_{||} < 1$

$\mathbf{\Gamma = (\sigma/\eta)\, q_{||}}$

overdamped wave

# Dynamics at Surfaces: Capillary Waves

X-Ray Photon Correlation Spectroscopy
in Surface Geometry

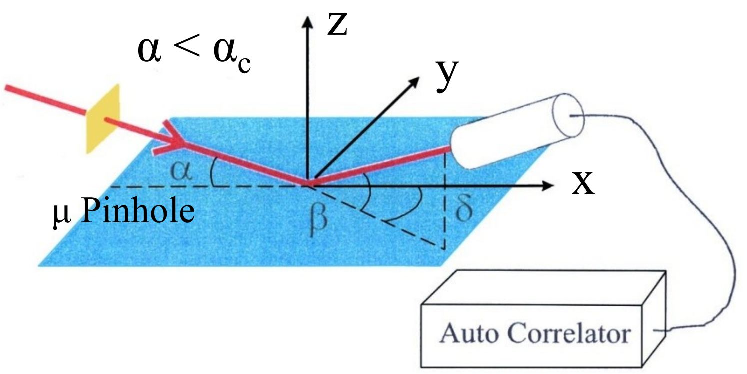


**$\alpha = \beta$ : reflectivity** **$q_z = (2\pi/\lambda)\, 2 \sin \alpha$**

**$\alpha_i = \alpha_c$ :** **50 - 100Å penetration**
**surface sensitivity**

**$\alpha \neq \beta$ :** **$q_{||} = 2\pi/\lambda(\cos \beta - \cos \alpha)$**
**in-plane correlations**

Glycerol: a „prototypical“ glassformer

Seydel, Madsen, Tolan, Grübel, Press, PRB63, 73409 (2001)

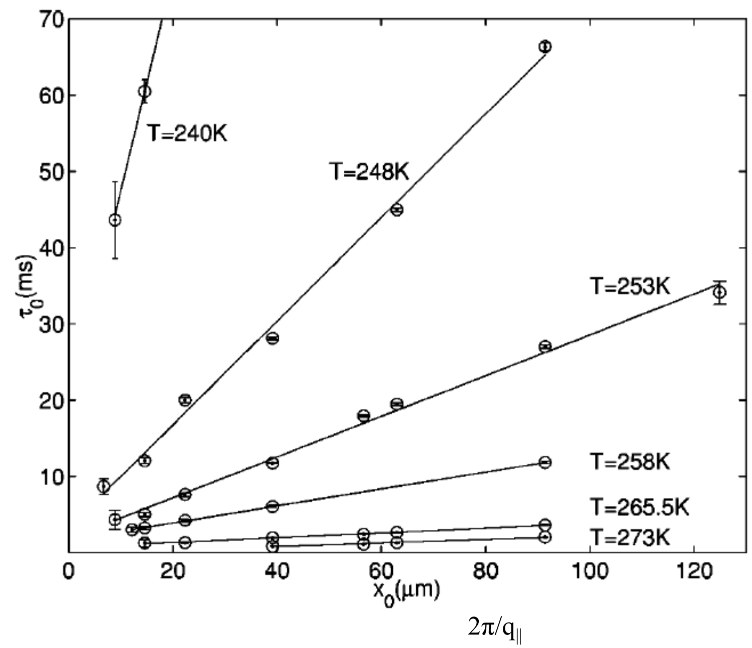


overdamped regime:

$\Gamma = (\gamma/2\eta)k; \qquad \tau_0 = \{\eta(T)/\pi\, \gamma(T)\}x_0$

# Viscosity of a liquid crystal near the nematic to smecticA transition

A. Madsen, J. Als-Nielsen and G. Grübel, PRL,90,85701(2003)

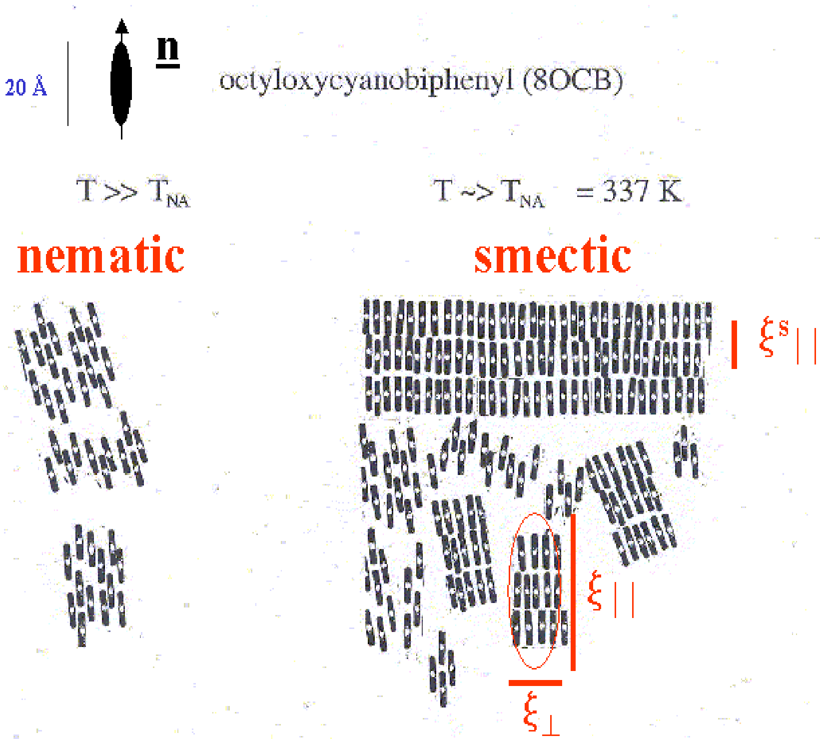


$$\xi_{\parallel} \sim \{(T - T_{NA})/T_{NA}\}^{\nu_{\parallel}} \quad = \quad \xi^{s}_{\parallel}$$

$$\xi_{\perp} \sim \{(T - T_{NA})/T_{NA}\}^{\nu_{\perp}}$$

$$\nu_{\parallel} = 0.71;\ \nu_{\perp} = 0.58$$

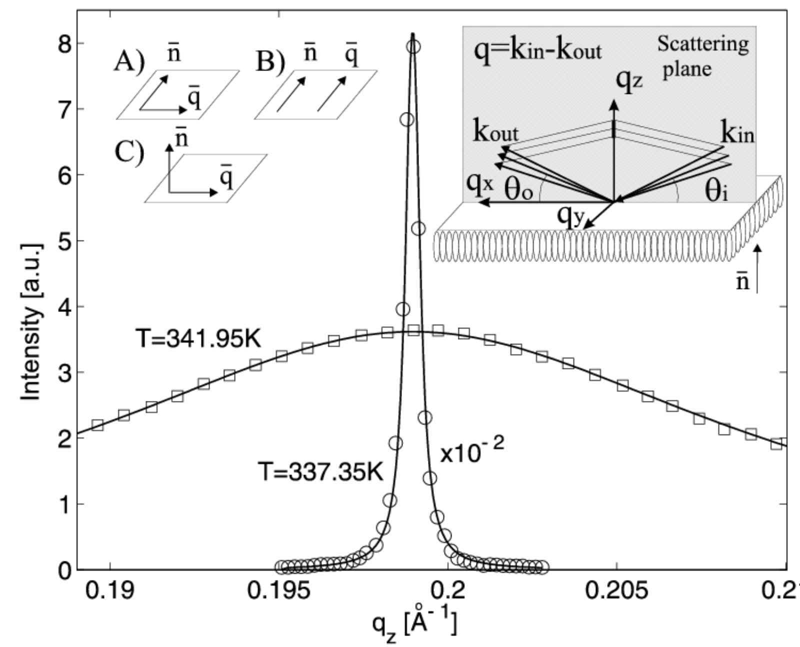


**References:** *Pershan and Als-Nielsen, PRL52,759(1984)*
*Pershan, Braslau,Weiss, Als-Nielsen, PRA35,4800(1987)*

# Viscosity of a Liquid Crystal near the Nematic-SmecticA Transition

Dynamics:

viscosity is anisotropic: $\eta_1, \eta_2, \eta_3$

depending on the relative orientations:

**n**, **v**, $\nabla$•**v**

described by Leslie coefficients $\alpha_1 \ldots \alpha_5$,
or parameters $\nu_1 \ldots \nu_5$ (Harvard notation)
($\nu_4 = \nu_5 = 0$ for incompressible fluids)

Theory: (N-SmA transition)

$$\eta_1 \sim \exp(E_A/kT)$$

$$\eta_2 \sim \exp(E'_A/kT)$$

$$\eta_3 = c(T-T_{NA}/T_{NA})^{-\beta} + \text{non.div.}$$

Predictions:

$\beta = 3\nu_{||} - 2\nu_{\perp}$ [1]

$\beta = 1/3$ [2]

$\beta = 1/2$ [3]


[1] Hossein, Swift, Chen, Lubensky, PRB19,432(1979)

[2] Jähnig,Brochard, J.Phys.,35,301(1974); deGennes, Sol. State Comm.,10,753 (1972)

[3] Langevin,J.Phys.37, 101(1975)

# Viscosity of a Liquid Crystal near the Nematic-SmecticA Transition

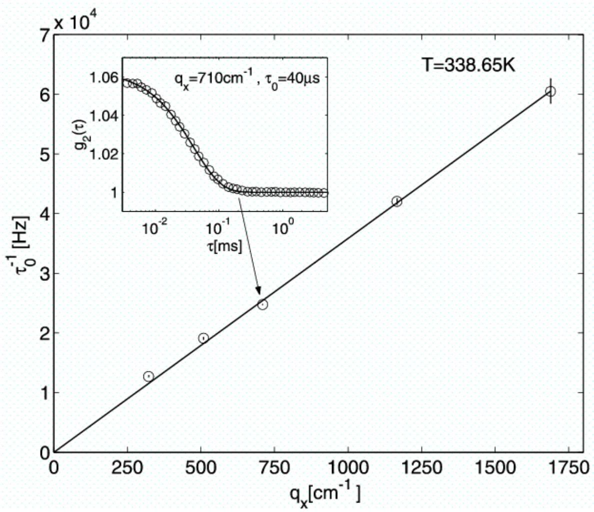


**XPCS: overdamped modes**

$\eta_3 \sim (T\text{-}T_{NA}/T_{NA})^{-\beta}$
$\beta = 0.95(2)$

<u>in agreement with theory [1]:</u>
$\beta = 3\nu_{||} - 2\nu_{\perp} = 0.94$
$\nu_{||} = 0.70;\ \nu_{\perp} = 0.58$ (static data)

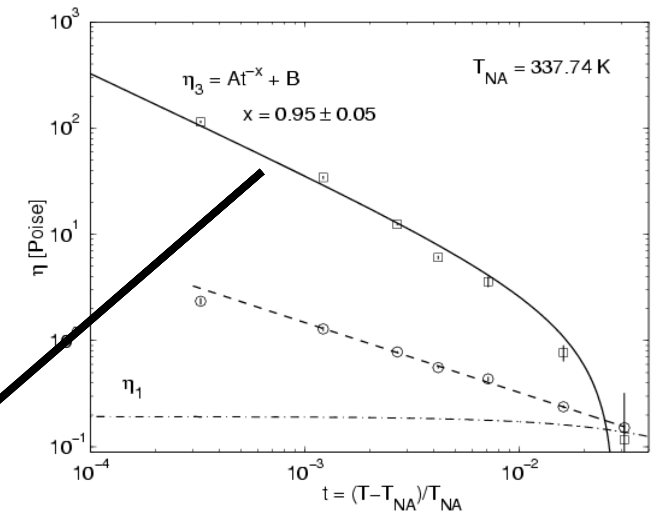


**$\eta$ / $\sigma$ diverging**
$\sigma$ constant [1]; data reflect temperature dependence of viscosity

- Out-plane movements ($\zeta$ || n) within the smectic layers are strongly damped ($\eta_3$ critical).
- The smectic layers remain viscous in-plane ($\eta_2$ non-critical)

# Non-Equilibrium Dynamics

Domain coarsening in phase separating systems (glasses, alloys,…) e.g. after quenching, aging…

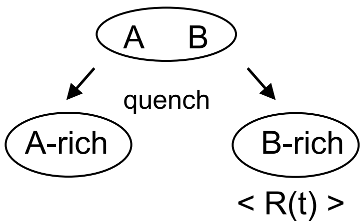


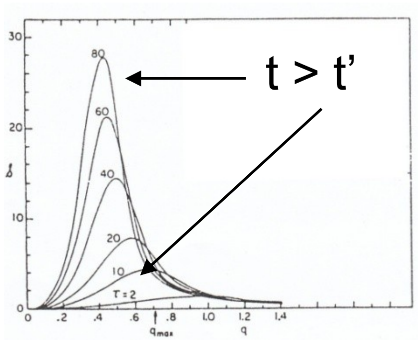


**Phase – separating Glass**

*Malik et al., PRL 81, 5832, 1998*

$(Na_2O)_{0.07}(B_2O_3)_{0.22}(SiO_2)_{0.71}$ T=1033K

quench

$(B_2O_3)$-rich $(SiO_2)$-rich 943K<T<963K

**Dynamic Scaling:** $\langle R(t) \rangle \sim t^n$

n=1/3 conserved order parameter (model B)

n=1/2 non-cons. order parameter (model A)

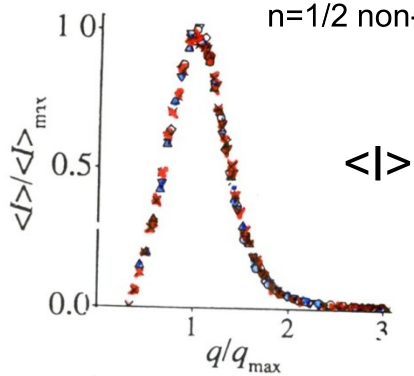


$$\langle I \rangle(q,t)/\langle I \rangle_{max} = F(q/q_{max})$$

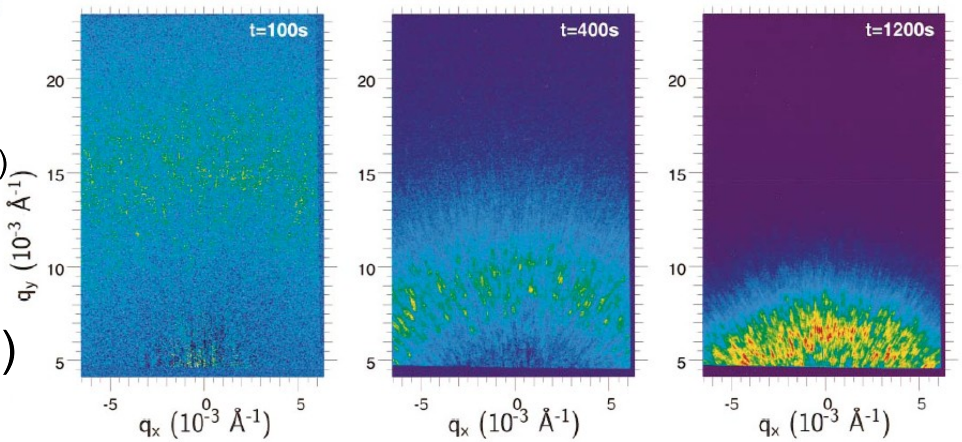


$\langle R(t) \rangle \sim t^n$ n=1/3

**XPCS:** investigate fluctuations around the average scaling behaviour: $\tau = \tau(q,t)$

# Two time correlation function:

$$C(q,t_1,t_2) = \frac{\langle I(t_1)\, I(t_2)\rangle - \langle I(t_1)\rangle \langle I(t_1)\rangle}{[\langle I^2(t_1)\rangle - \langle I(t_1)\rangle^2]^{1/2}\, [\langle I^2(t_2)\rangle - \langle I(t_1)\rangle^2]^{1/2}}$$

Fluctuations $\tau = \tau\,(q,t)$

**Prediction:** Brown et al. PRE 56,6601,1997

$\Delta t = t_1 - t_2$

$$\bar{t} = \frac{t_1 + t_2}{2}$$

$$\tau\,(q,t) = [t_{max}(q)-t_o]\,\{\underbrace{a\,[t-t_o]\,/\,[t_{max}(q)-t_o]}_{x}\}^{(1-n)}$$

$\sim 1/q \;\; t^{2/3}$

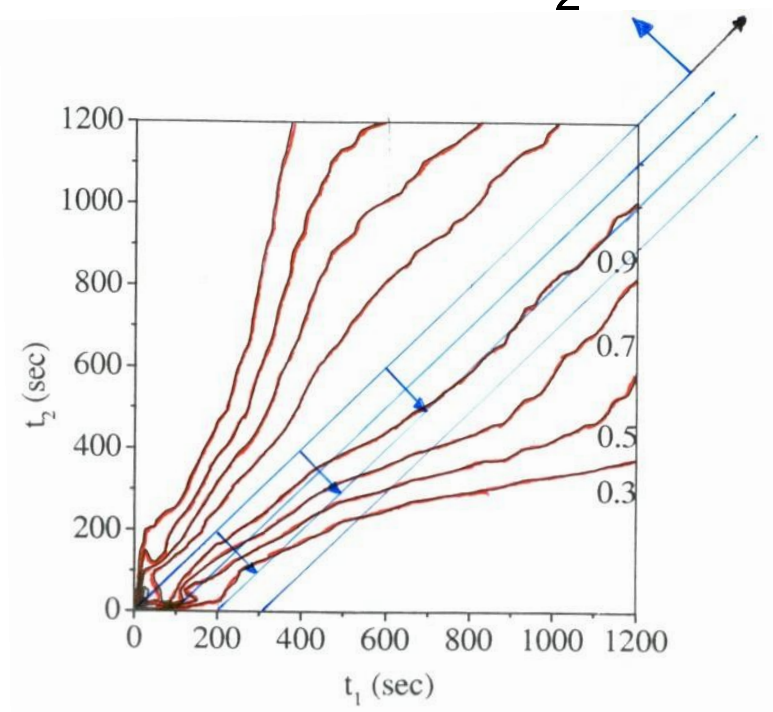


$\tau = \tau\,(t)$

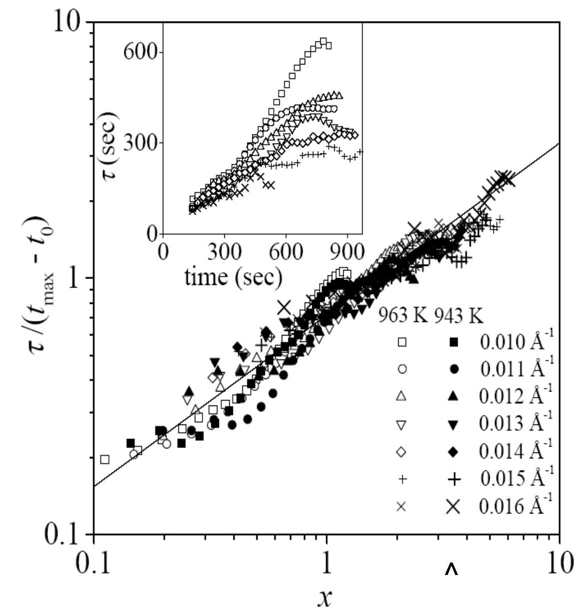


$a = 0.72(2)$  $(1-n) = 0.65(4)$  $= 1 - ⅓$

# Phase-Ordering in $Cu_3Au$

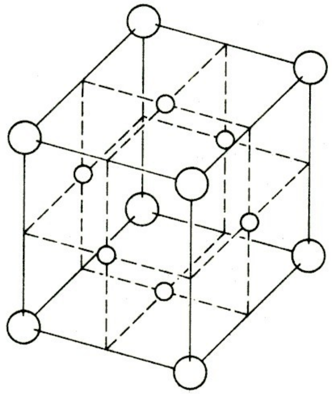

high T: fcc sites occupied by either Cu or Au

T≤Tc=383 C: ordering with Au on corner and Cu on face sites

4-fold degenerate ground-state

(corners can be choosen in 4 different ways)

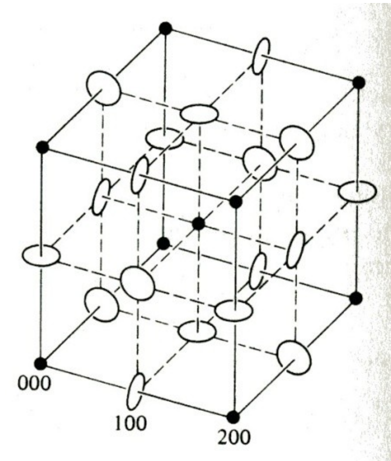


groundstates separated by domain walls

domain walls give rise to ellipse shaped superlattice reflections of type [100]

quench: domain formation and growth in disordered phase
domain coarsening with $R \sim t^{1/2}$

[100] superlattice reflection after quench from 425 C to 370 C

**Fluerasu&Sutton, PRL94(2005)55501**

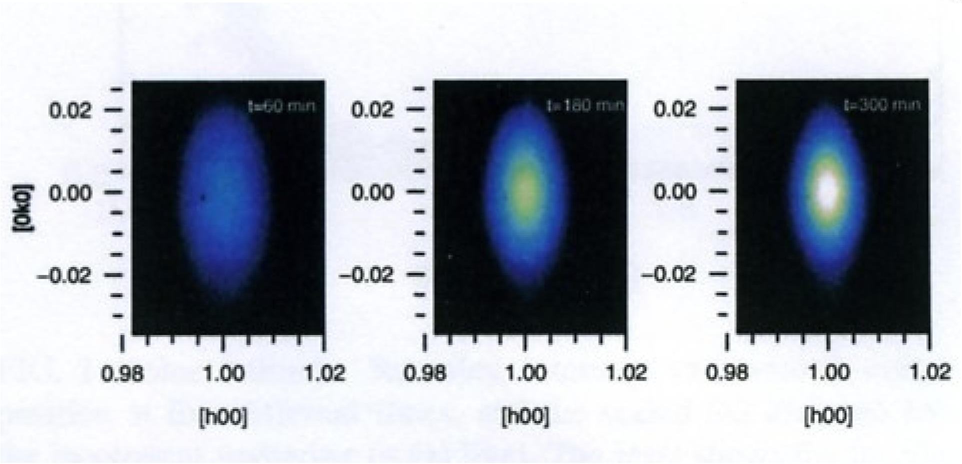


 

- Study fluctuations about the average behaviour: XPCS

characterize by two-time correlation function

$$C(q,t_1,t_2) = \frac{<I(t_1)\, I(t_2)> - <I(t_1)> <I(t_1)>}{[<I^2(t_1)> - <I(t_1)>^2]^{1/2}\, [<I^2(t_2)> - <I(t_1)>^2]^{1/2}}$$

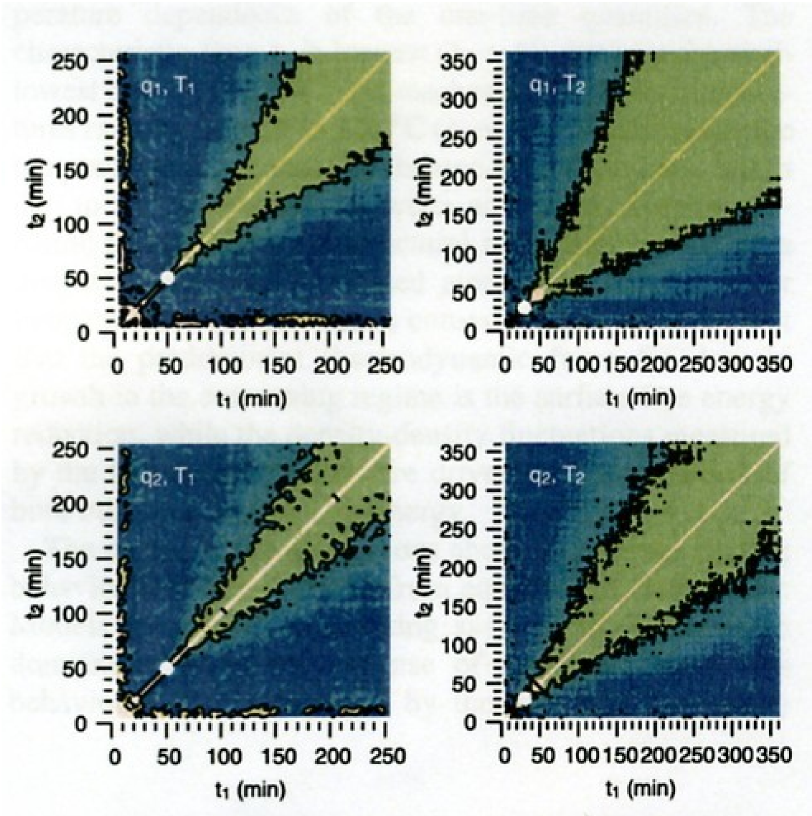

- rescaled correlation time $\tau \sim t_{mean}$ in the low $t_{mean}$ limit

  $\sim t_{mean}^{1/2}$ in the high $t_{mean}$ limit

  with dq = Q - [100]

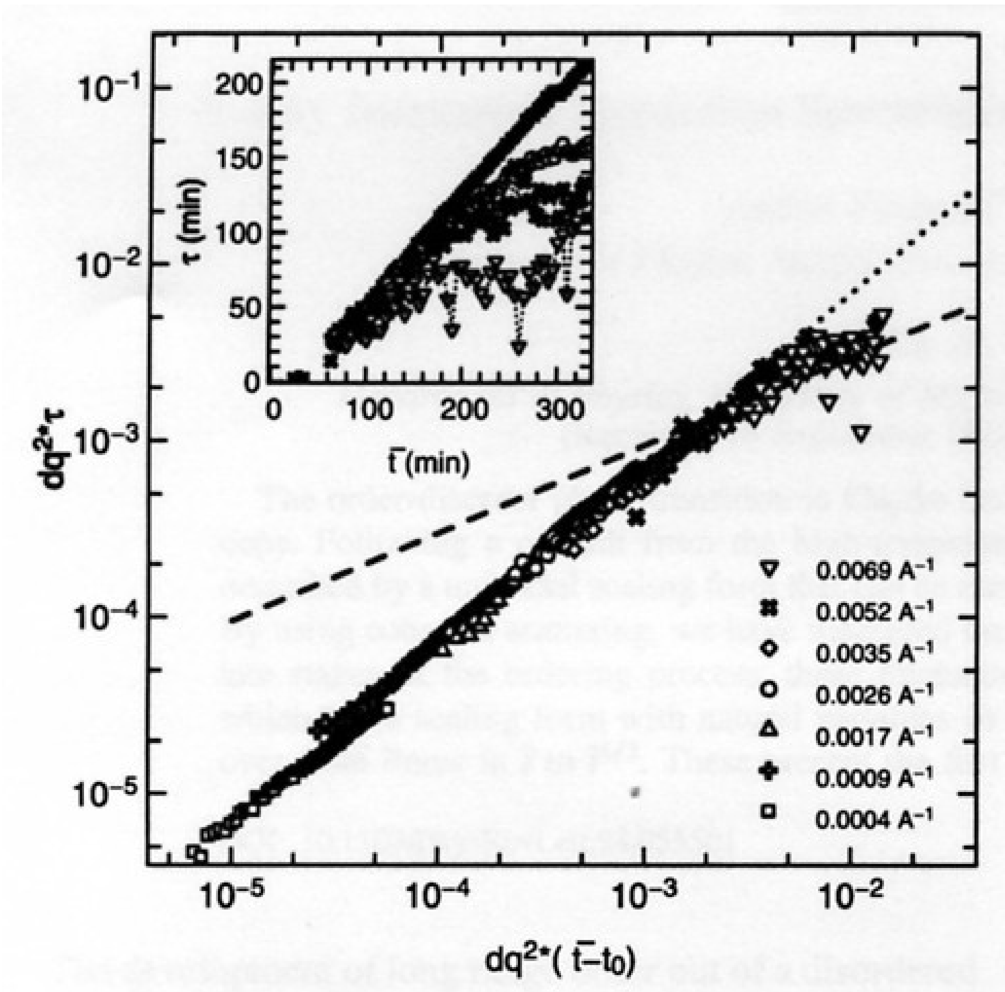


 

# XPCS – operating range

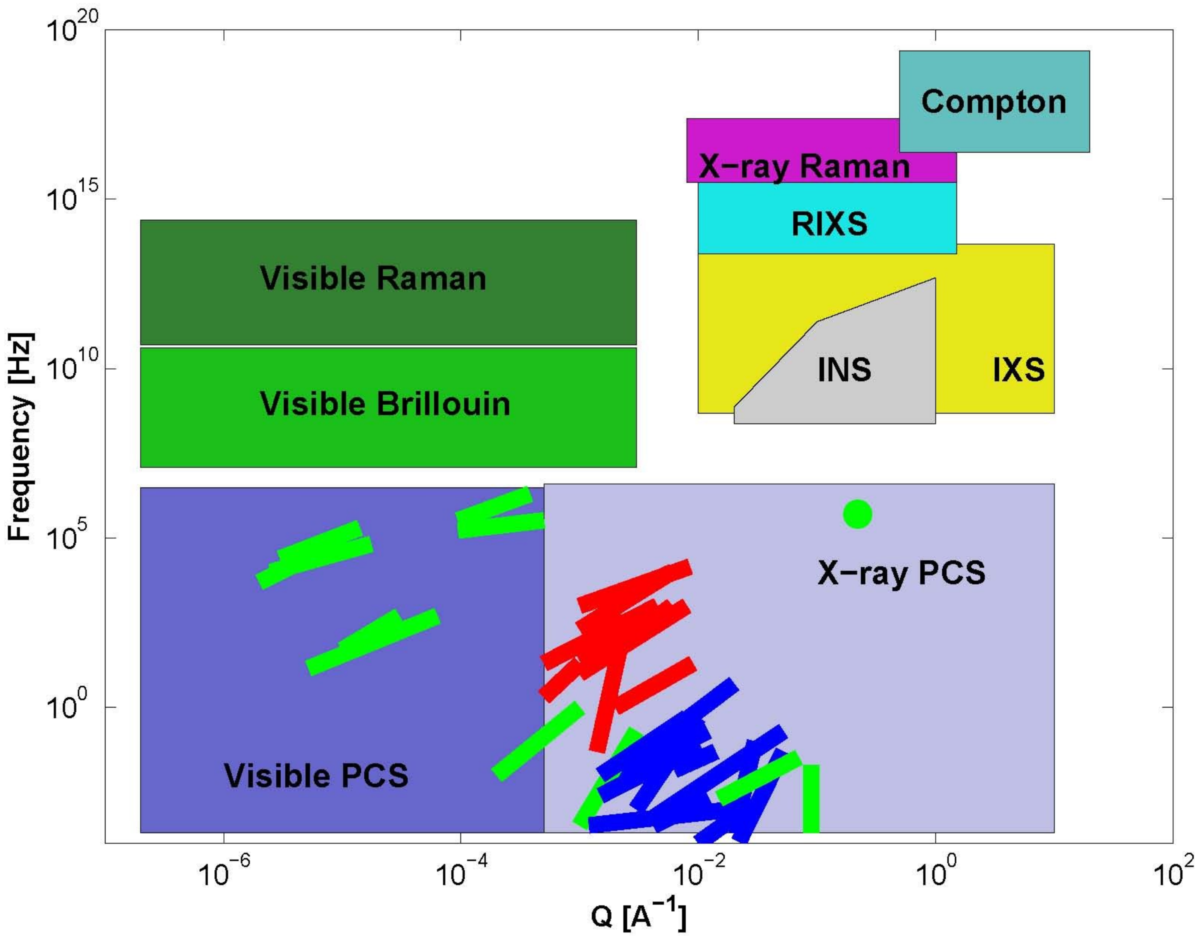


## XPCS

- access to large momentum transfers ($Q_{max}=2\pi \bullet \sin\theta/\lambda$) or short lengthscales
- not subject to multiple scattering
- can be combined with the surface sensitivity of X-rays

▪

# Imaging and XPCS at an FEL source

Fc = $(\lambda/2)^2 \bullet$ B(rilliance) B (storage ring) ≈ $10^{20}$ - $10^{21}$

Length of a storage ring pulse ≈ 50-100 ps

# (X)FEL key parameters

- <u>X-ray FEL radiation (0.2 - 14.4 keV)</u>
  - **ultrashort pulse duration** **100 fs**
  - **extreme pulse intensities** **$10^{12}$-$10^{14}$ ph**

  - **coherent radiation** **x$10^9$**
  - **average brilliance** **x$10^4$**

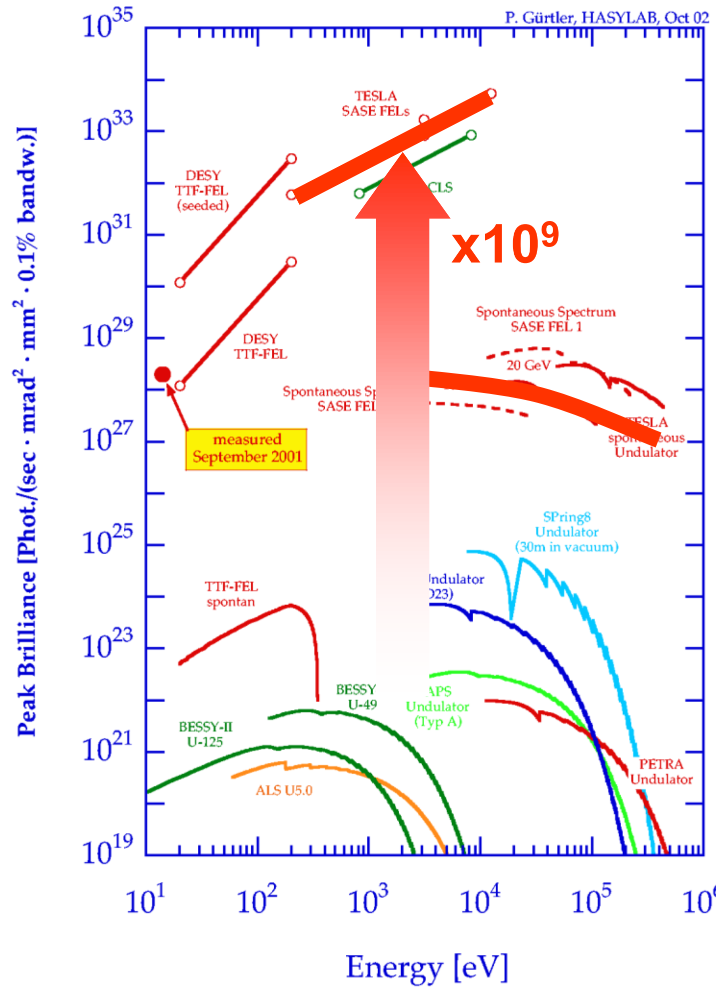


 

# LINAC driven SASE free-electron laser

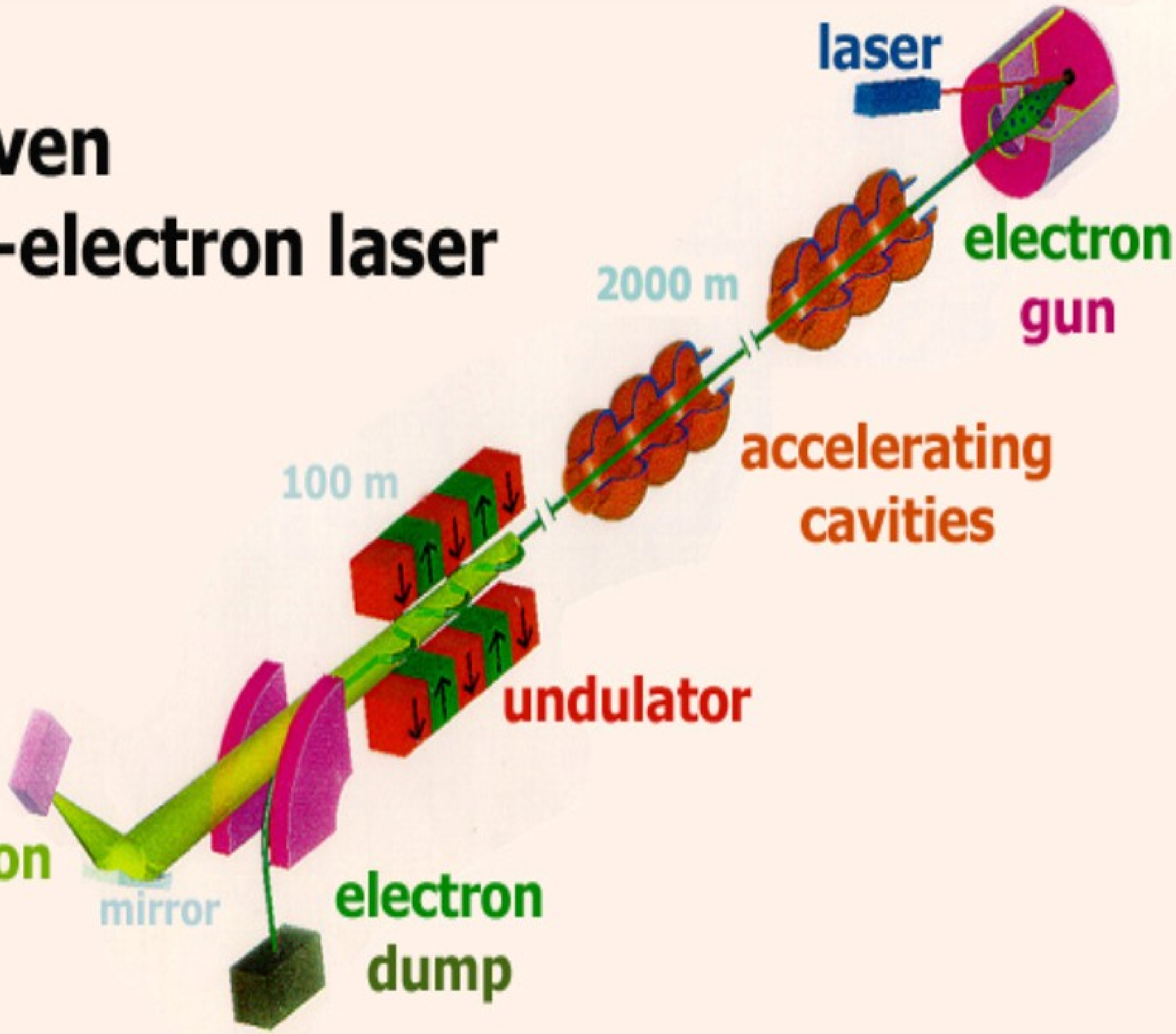

## Dipole magnet
## synchrotron radiation

dF ~ $E^2$ I

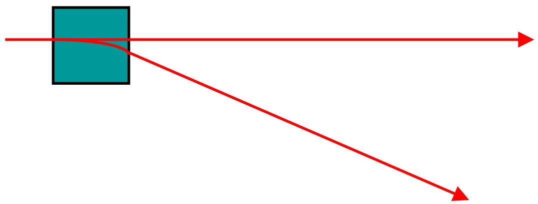

## Wiggler

~ 2N $E^2$ I

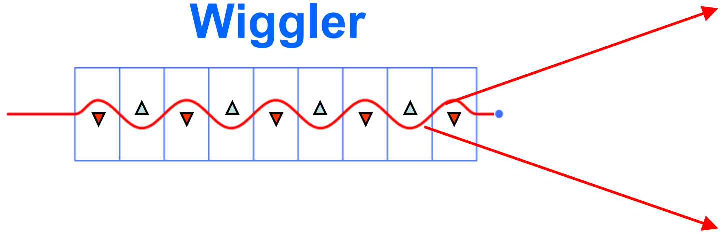

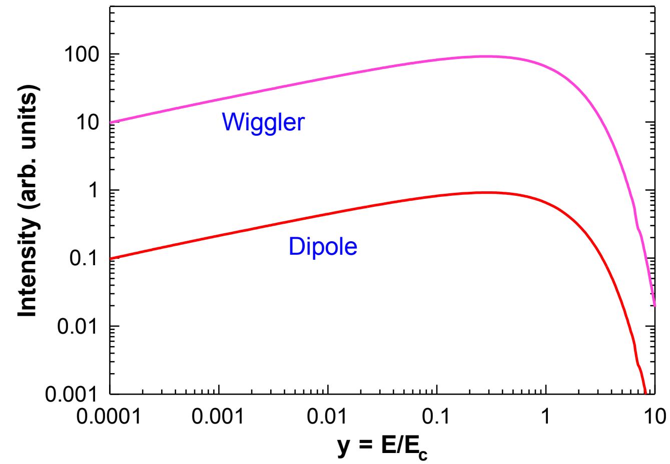


## Undulator

~ $N^2$ $E^2$ I

~ $n_e$

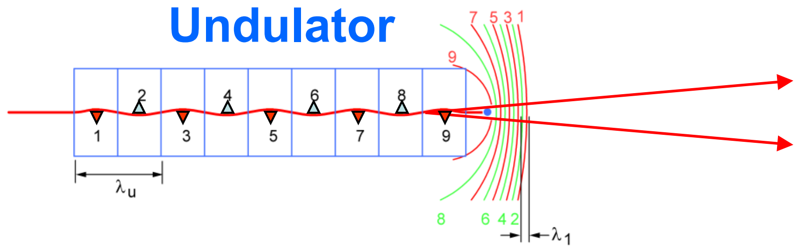


The radiation emitted by a single electron in subsequent oscillations in an undulator is in phase. Radiation from different electrons is NOT (positional disorder in bunch).

## FEL

~ $n_e^2$

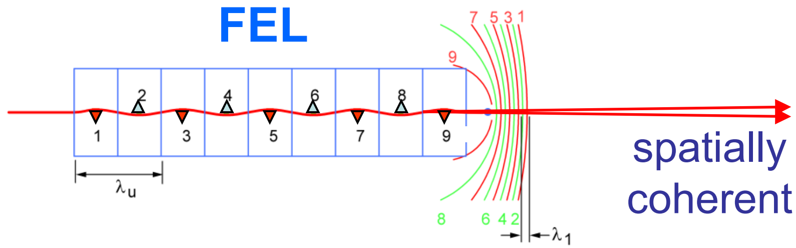


spatially coherent

"Phasing" is achieved via positional order in the bunch (micro-bunching) with a period equal to the x-ray wavelength.

# SASE (self-amplified spontaneous emission)

**Idea: Send a perfect electron beam through a very long undulator using the spontaneous radiation as a seed**

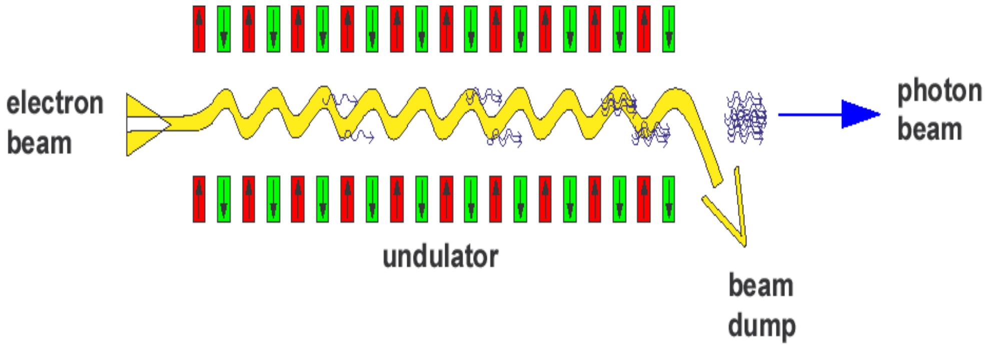


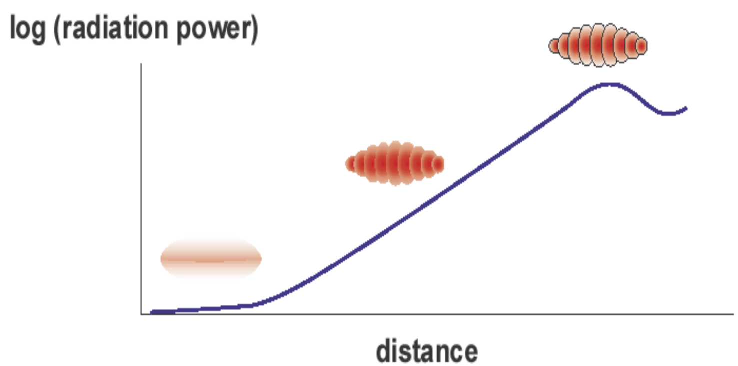


A.M. Kondratenko, E.L. Saldin, Part. Acc. **10**, 207 (1980)
*Generation of coherent radiation by a relativistic electron beam in an ondulator*
R. Bonifacio, C. Pellegrini, L. Narducci, Opt. Commun. **50**, 373 (1984)
*Collective instabilities and high-gain regime in a free electron laser*

# Simulation

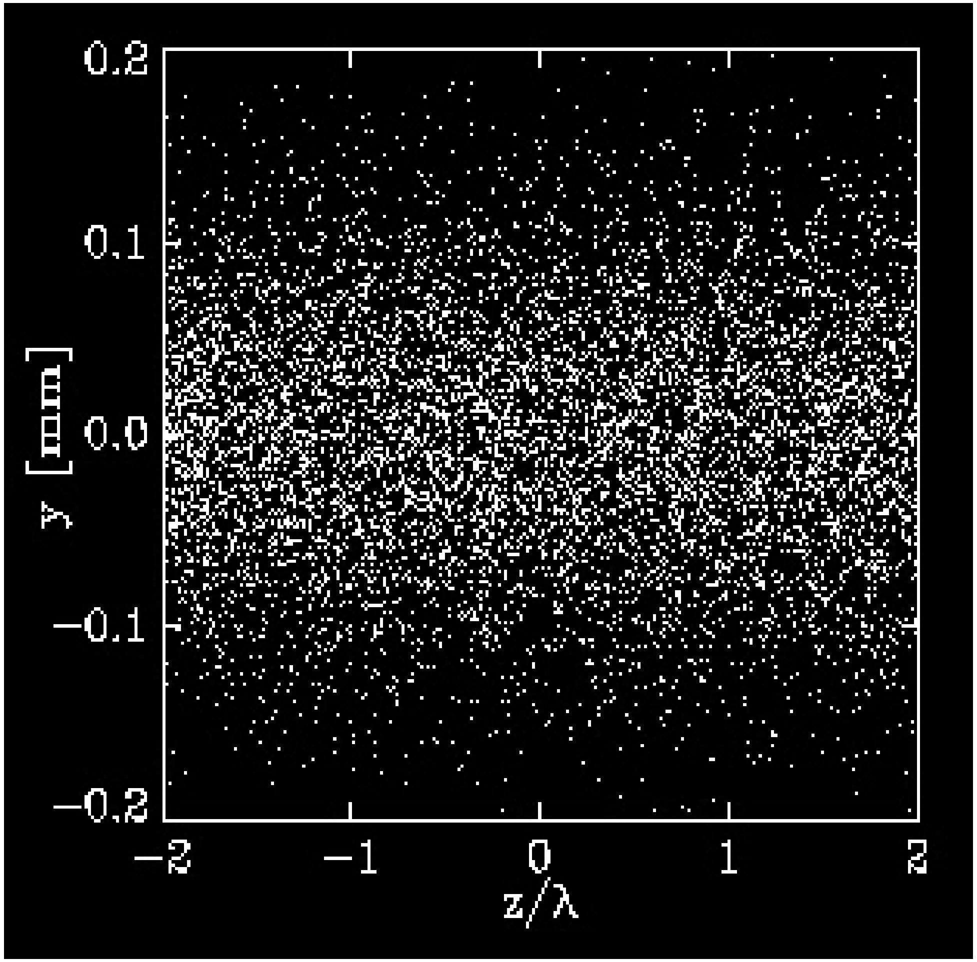


GENESIS – simulation for TTF parameters

Courtesy Sven Reiche (UCLA)

# Time Structure and Coherence Properties of XFEL radiation

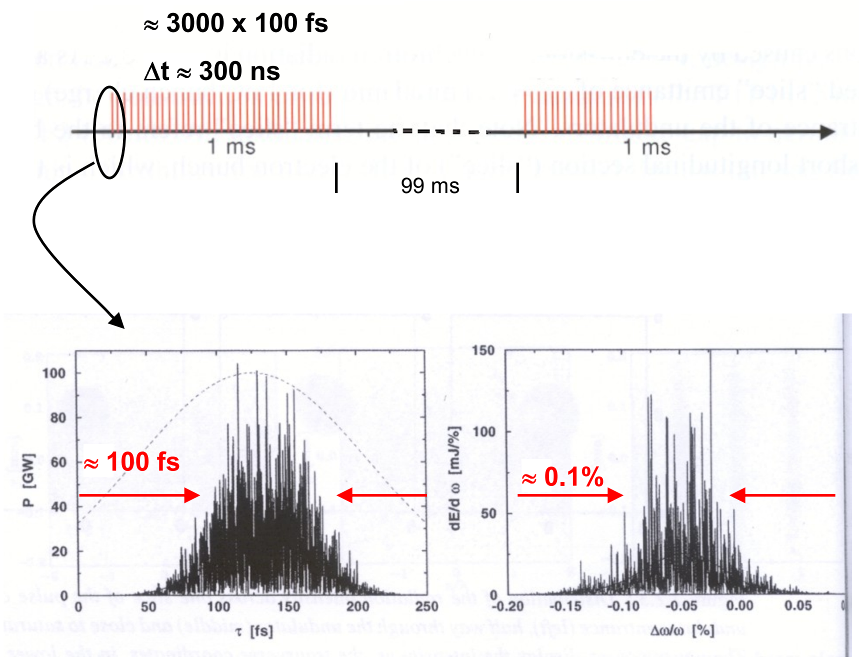


#ph/mode ≈ $10^9$ = #ph/bunch / M(# modes)

= $10^{12}$ / 1000

M < 1000

for $\Delta\lambda/\lambda$ / N(=1000) = $10^{-6}$:

Get single spatially and temporally coherent wave packet carrying about $10^9$ photons.

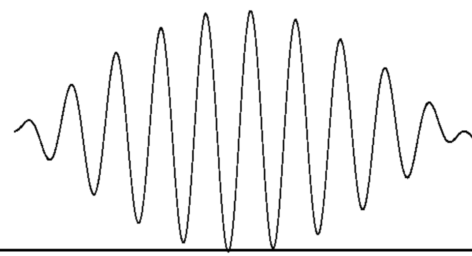

<u>Pulse-to-pulse statistics:</u>

M=1: single mode
strong pulse-to-pulse fluctuations

M>1: multi-mode

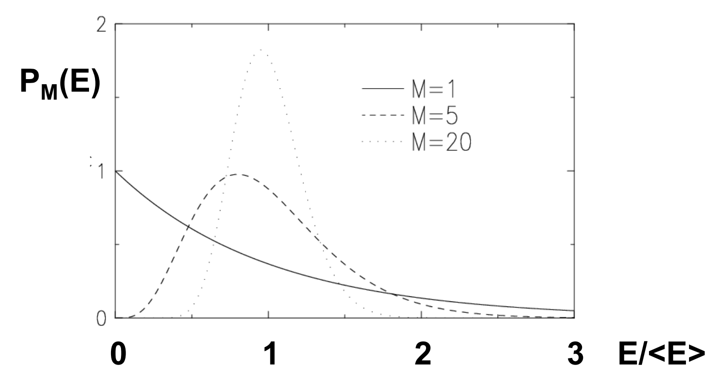

# The FLASH facility

$\lambda \geq 4.5$ nm

*Commissioning: 2004/5*

*User experiments: 2005*

# FLASH Overview

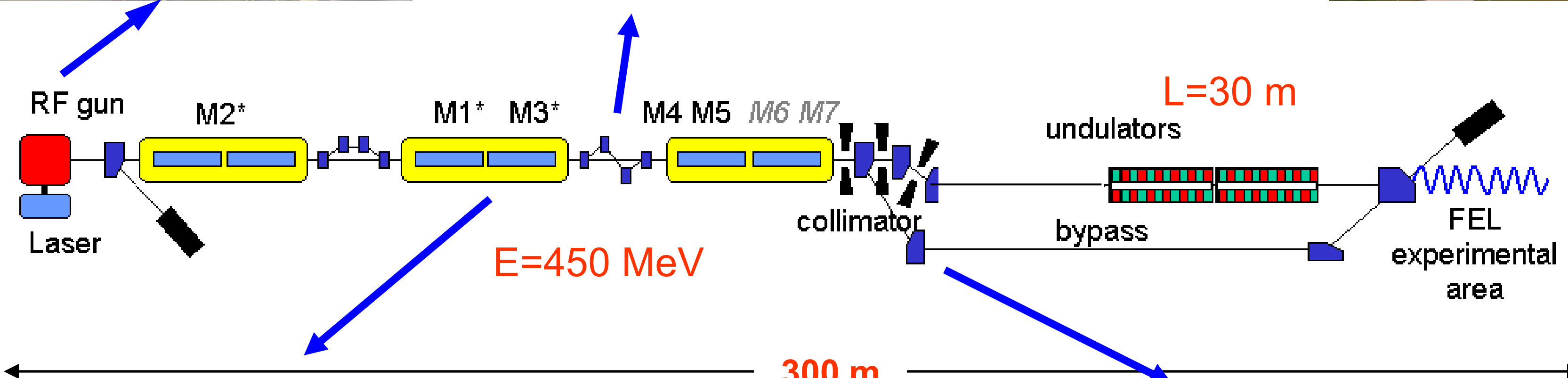


- Jan 2005: first lasing at 32 nm
- Aug 2005: first user exper.

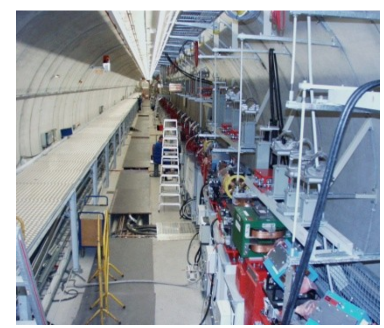

# FLASH Performance

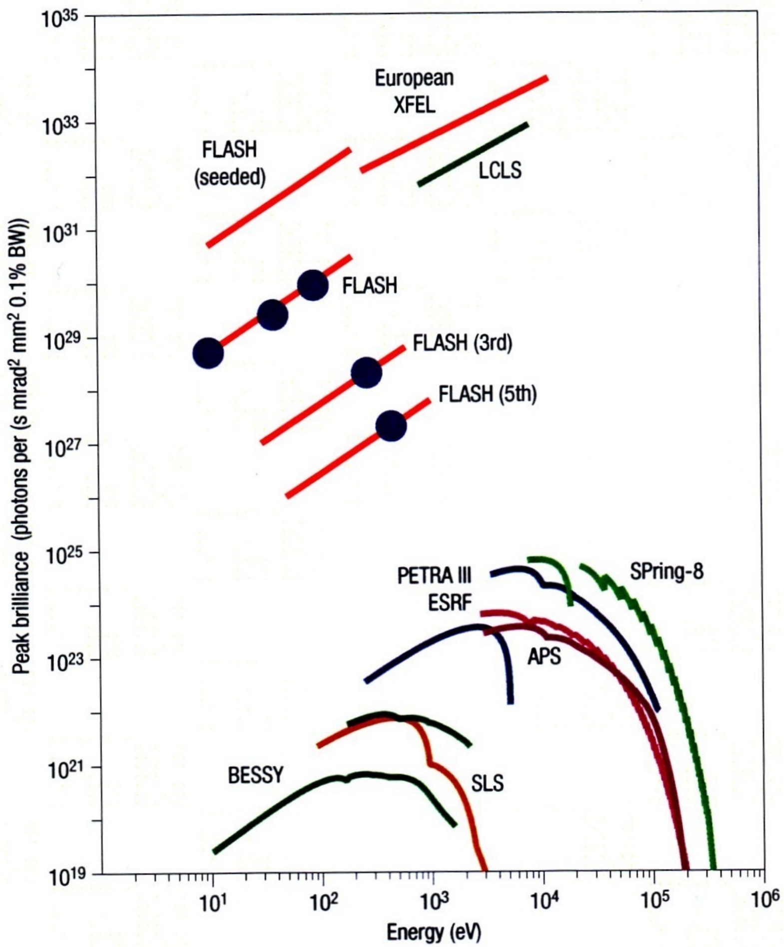


FLASH performance:

pulse duration ≤ 20 fs

1st 13.7 nm $B_{peak}$ =6•$10^{29}$

3rd 4.6 nm $B_{peak}$ =2•$10^{28}$

5th 2.75 nm $B_{peak}$ =2•$10^{27}$

# Double Slit Diffraction at FLASH

λ = 100 nm

d=0.5mm

d=1mm

d=2mm

d=3mm

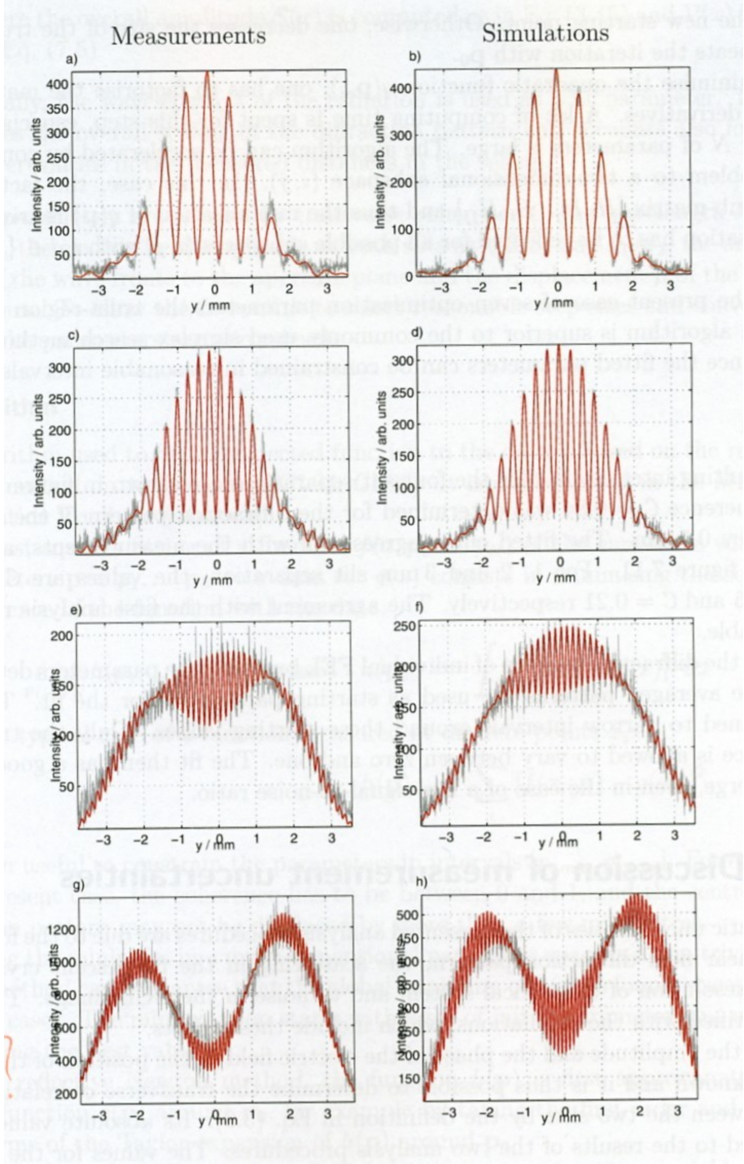


Thesis Rasmus Ischebeck

# ▪ Double Slit Diffraction at FLASH

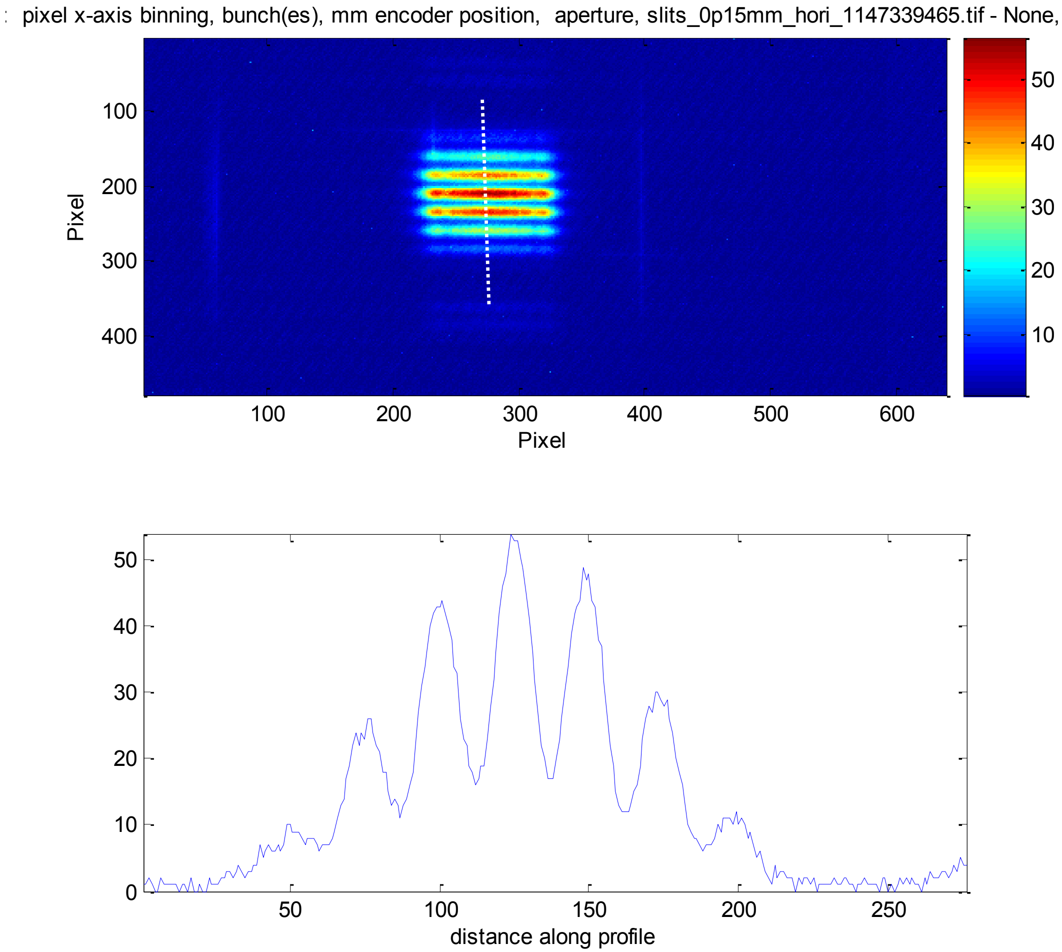


R. Treusch
M. Kuhlmann

Wavelength λ= 25.6 nm, Slits separation 0.15 μm, Image is a sum of 10 FEL pulses

▪

# Imaging at a FEL

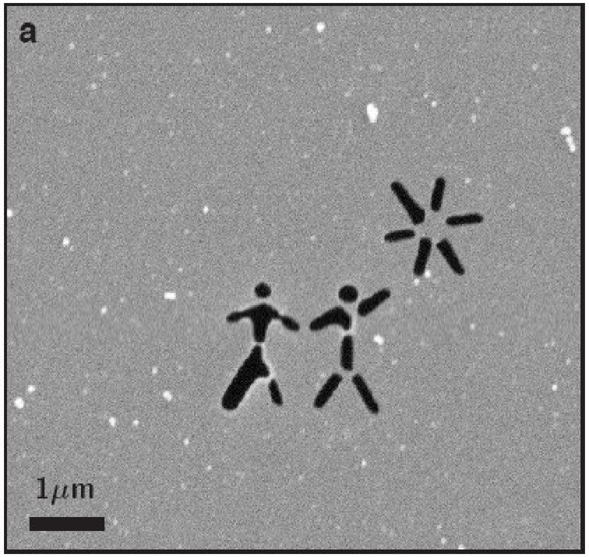


Model structure in 20 nm SiN membrane

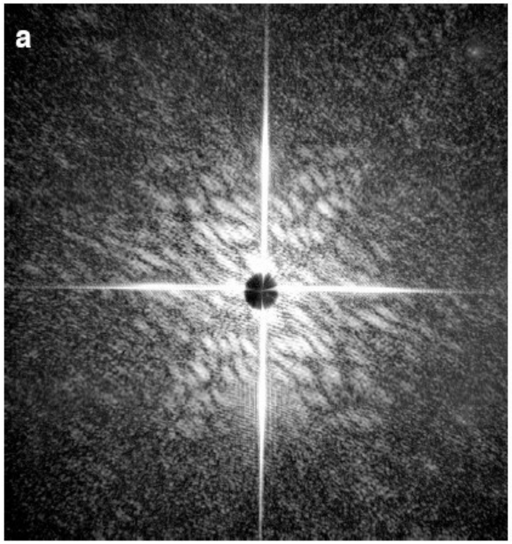


Speckle pattern recorded with a single (25 fs) pulse

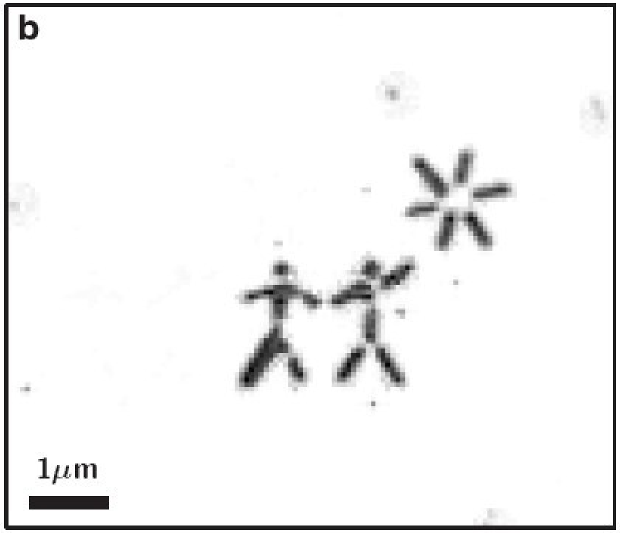


Reconstructed image

*Incident FEL pulse:*
*25 fs, 32 nm,*
*4 x $10^{14}$ W $cm^{-2}$ ($10^{12}$ ph/pulse)*

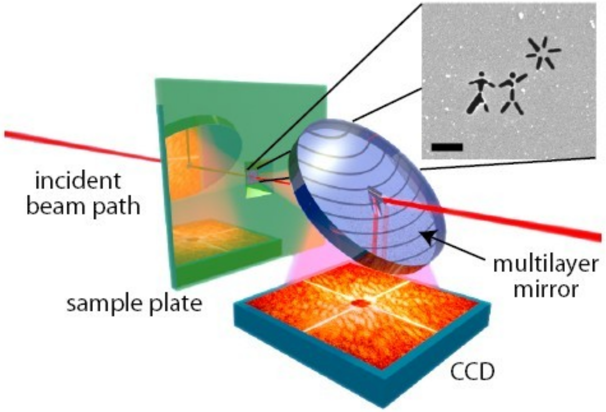


H. Chapman et al., Nature Physics, 2,839 (2006)

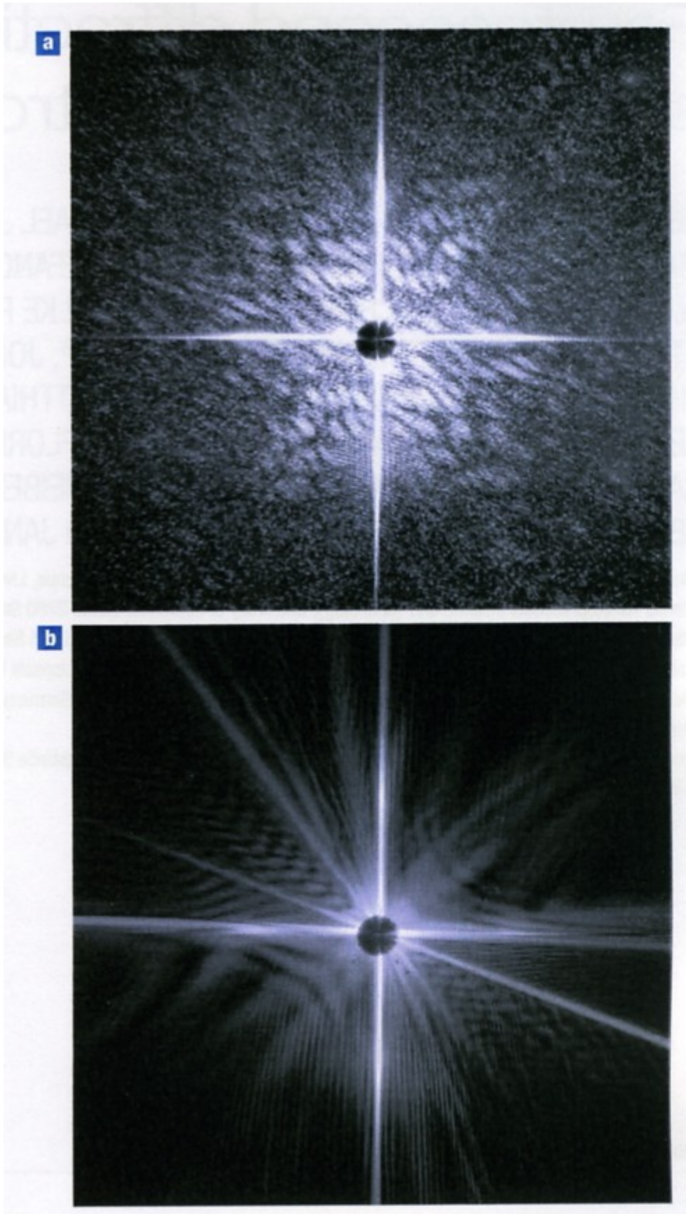


model structure

***First FEL pulse:***
***25 fs, 32 nm,***
***$4 \times 10^{14}$ W cm$^{-2}$***
***($10^{12}$ ph/pulse)***

“destroyed” model structure

***Second FEL pulse:***
***25 fs, 32 nm,***
***$4 \times 10^{14}$ W cm$^{-2}$***
***($10^{12}$ ph/pulse)***

# An approach to three-dimensional structures of biomolecules by using single-molecule diffraction images: A simulation

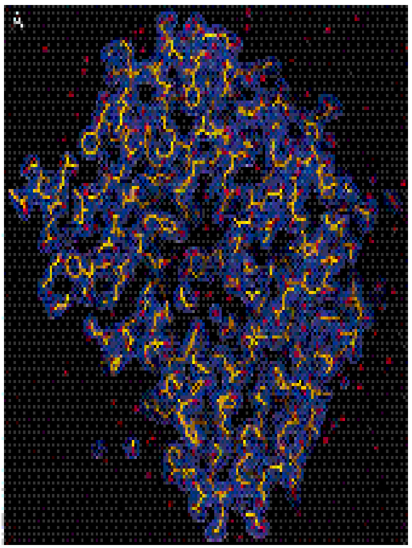

3-D structure (2.5 Å resolution) of rubisco molecule.

(106 kDa)

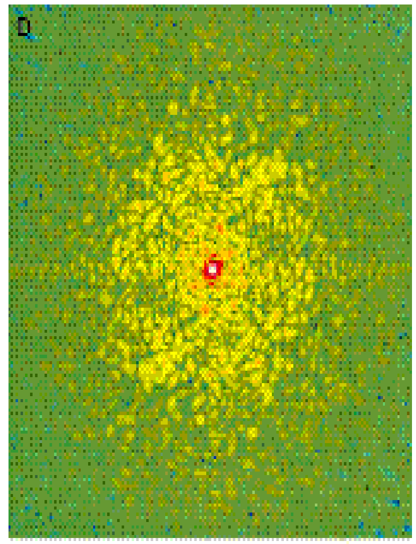

Top view of a section (kz=0) of 3-D scattering pattern from $10^6$ single molecules (of known relative orientation) each "exposed" by a single 10 fs XFEL pulse ($\lambda$=1.5Å, 0.1$\mu$m beamsize) containing $2 \cdot 10^{12}$ photons.

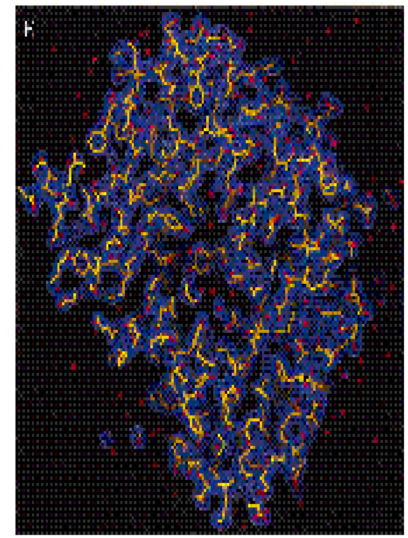

Reconstructed 3-D pattern (from 250 2-D projections). Phasing by "oversampling" technique.

J. Miao, K.O. Hodgson and D. Sayre, PNAS, 98, 6641 (2001)

**<u>NOTE:</u> Radiation Damage**

# Beam – Sample Interaction

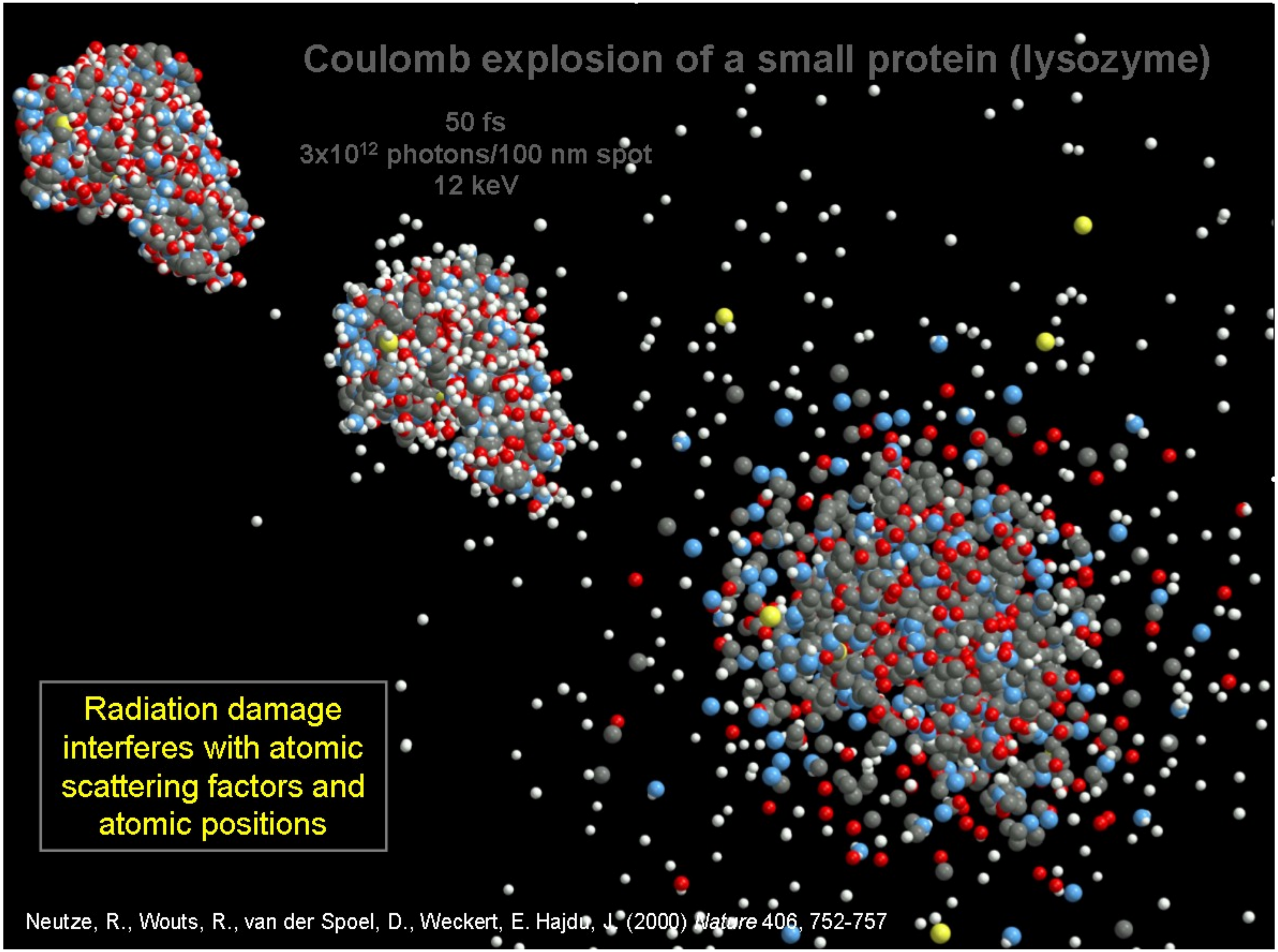

# Magnetic Small Angle Scattering at FLASH (1)

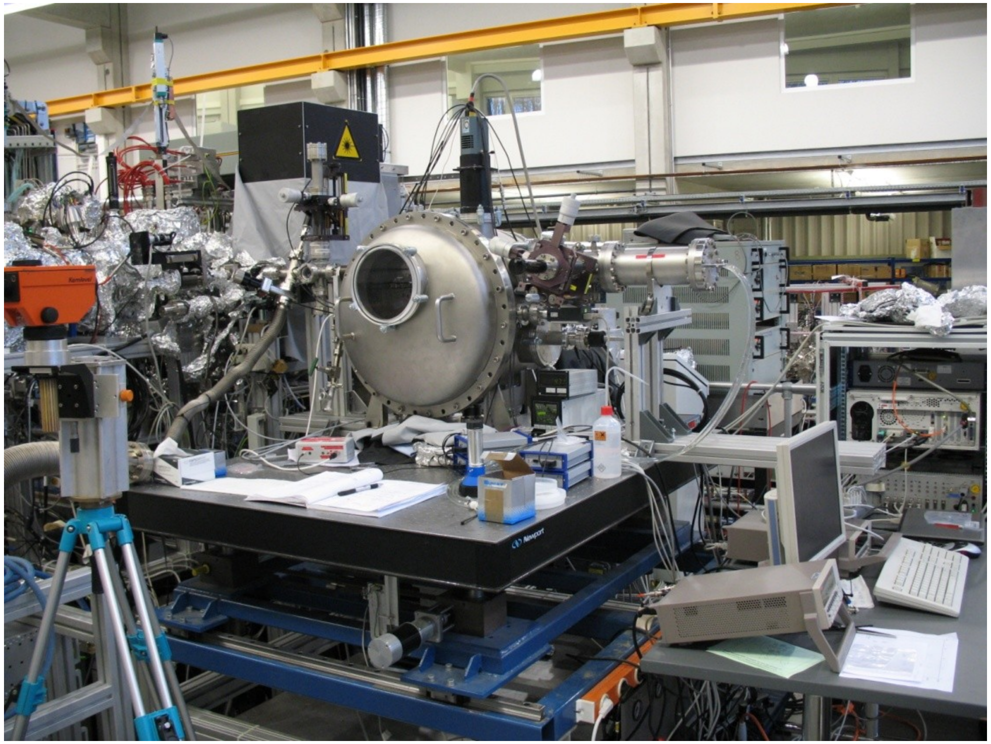

Magnetic Small Angle Scattering:

50 [Co(4Å) / Pt(7Å)] sputtered on 20nm Pt layer on $Si_3N_4$ membrane, capped with 2nm Pt

FLASH operation 19.12.2007:

SASE on 5th harmonic of 7.97 nm = 1.59 nm $\equiv$ 778 eV


L.-M. Stadler1, S. Streit-Nierobisch1, C.Gutt1, A. Mancuso1, A. Schropp1, J. Gulden1, B. Reime1, I.Vartaniants1, E. Weckert1, B. Pfau2, C.M. Günther2, R. Könnecke2, S. Eisebitt2, O. Hellwig3, F. Staier4, A. Rosenhahn4, T. Wilhein5, D. Stickler6, H. Stillrich6, R. Frömter6, H.P. Oepen6, R. Treusch1, N. Guerassimova1, M. Martins7, K. Honkavaara1, B. Faatz1, S. Schreiber1, M.V. Yurkov1, E.A. Schneidmiller1, A. Brenger1, and G. Grübel1

1 Deutsches Elektronen-Synchrotron DESY, Notkestraße 85, D-22607 Hamburg, Germany
2 Berliner Elektronenspeicherring BESSY – Gesellschaft für Synchrotronstrahlung, Albert-Einstein-Straße 15, D-12489 Berlin, Germany
3 Hitachi Global Storage Technology, 650 Harry Road, San Jose, CA 95120, USA
4 Institut für Physikalische Chemie, Universität Heidelberg, Im Neuenheimer Feld 229, D-69120 Heidelberg, Germany
5 Institute for Xray-Optics, RheinAhrCampus Remagen, FH Koblenz, Südallee 2, 53424 Remagen, Germany
6 Institut für Angewandte Physik, Universität Hamburg, Jungiusstraße 11, D-20355 Hamburg, Germany
7 Institut für Experimentalphysik, Universität Hamburg, Luruper Chaussee 149, D-22761 Hamburg, Germany

# Magnetic Small Angle Scattering at FLASH (2)

meandering magnetic stripe domain of a CoPt multilayer

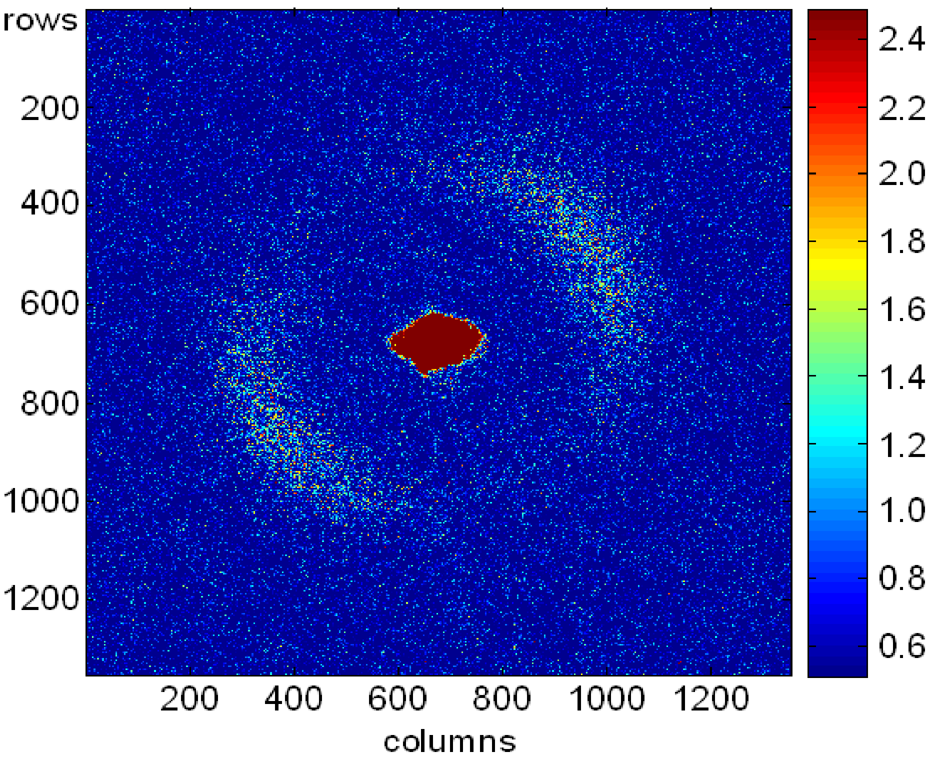


**Magnetic SAXS pattern:**

**E = 778.1 eV**

**ON (Co $L_{III}$) resonance**

▪

# Time-dependent Imaging and XPCS at a FEL

# Time delay holography (1)

H.N. Chapman et al., Nature 448(2007)676

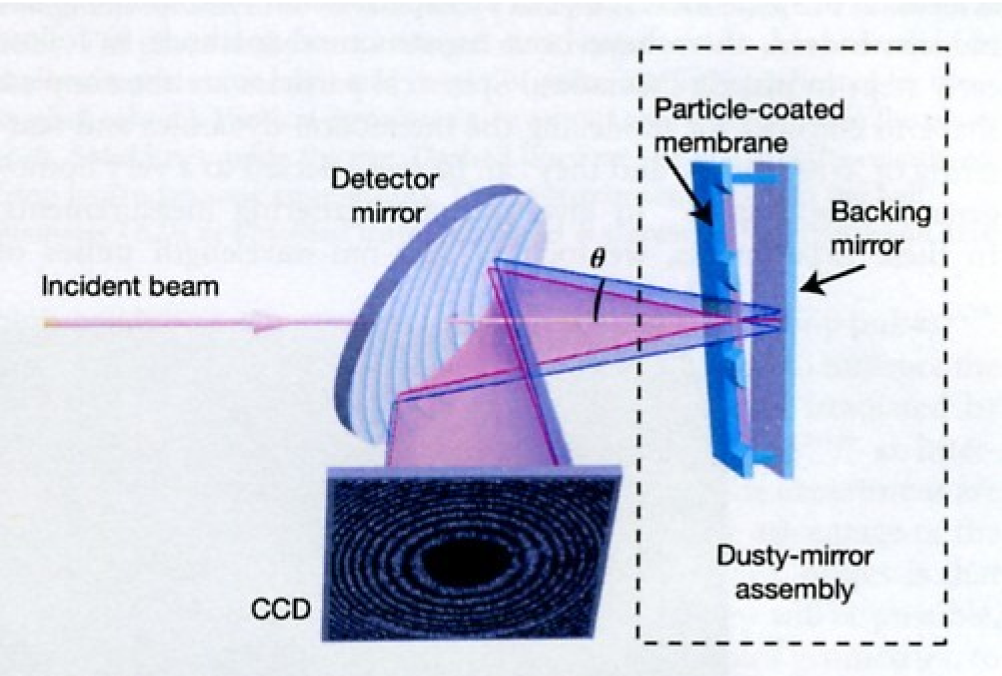


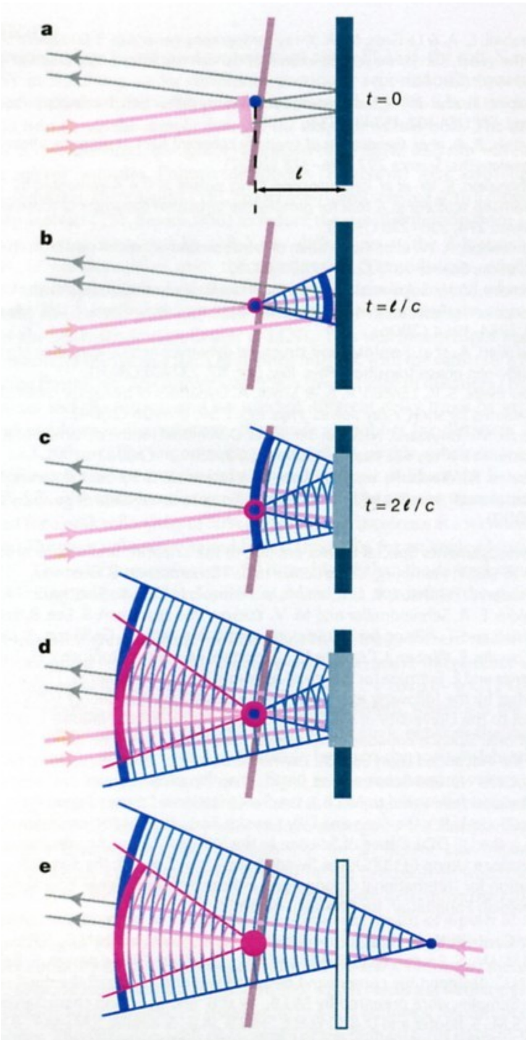


**25 fs long single pulses (≈$10^{12}$ ph/pulse) of 32.5 nm light from FLASH impinging on a particle coated (140 nm polystyrene PS particles) $Si_3N_4$ membrane.**

***The primary diffraction pattern (blue) interferes with the secondary (red) diffraction pattern arising from the (incident) beam being backreflected by a mirror and diffracted after a time delay $\Delta t$ from the "exploding" PS particles.***

# Time delay holography (2)

λ=32.5 nm
25 fs duration
$0.5 \bullet 10^{14}$ W/cm$^2$

$\Delta t$ = 348 fs

$\Delta t$ = 733 fs

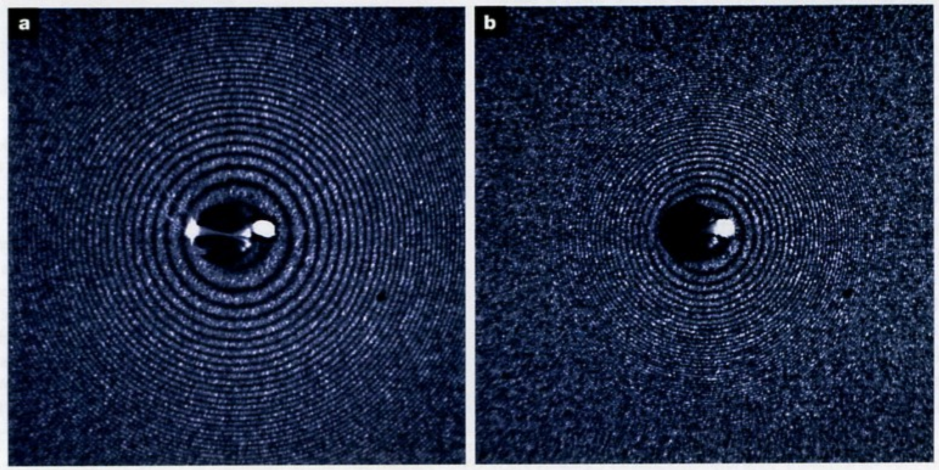


**Figure 2 | Time-delay X-ray holograms of 140-nm-diameter polystyrene spheres.** The time delays were $348 \pm 1$ fs (**a**) and $733 \pm 2$ fs (**b**). The pulses were 32-nm wavelength, 25-fs duration with intensities $(0.5 \pm 0.2) \times 10^{14}$ W cm$^{-2}$. The intensities of the holograms are shown on a linear greyscale, to a half-width of 4.5 μm$^{-1}$. We derive the time delays and the change in optical path through the exploding particles from the fringe pattern. The particle sizes are determined from the envelope of the intensity.

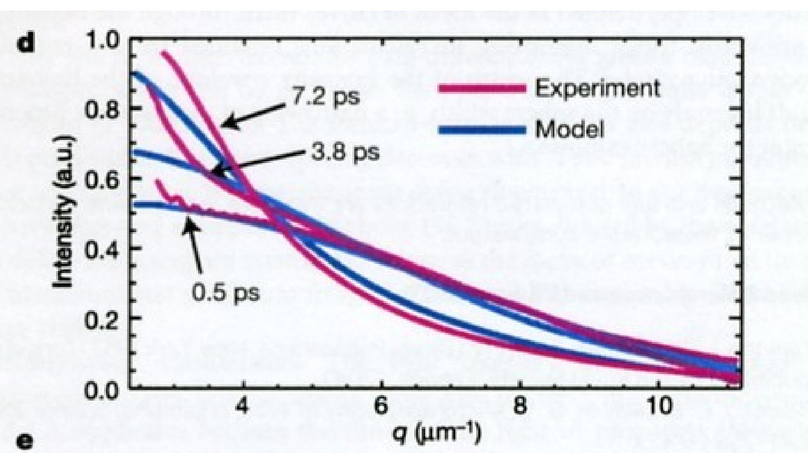


The intensity envelope of the interference pattern evolves to lower q indicating increasing radii of the particles.

# XPCS at a XFEL source:

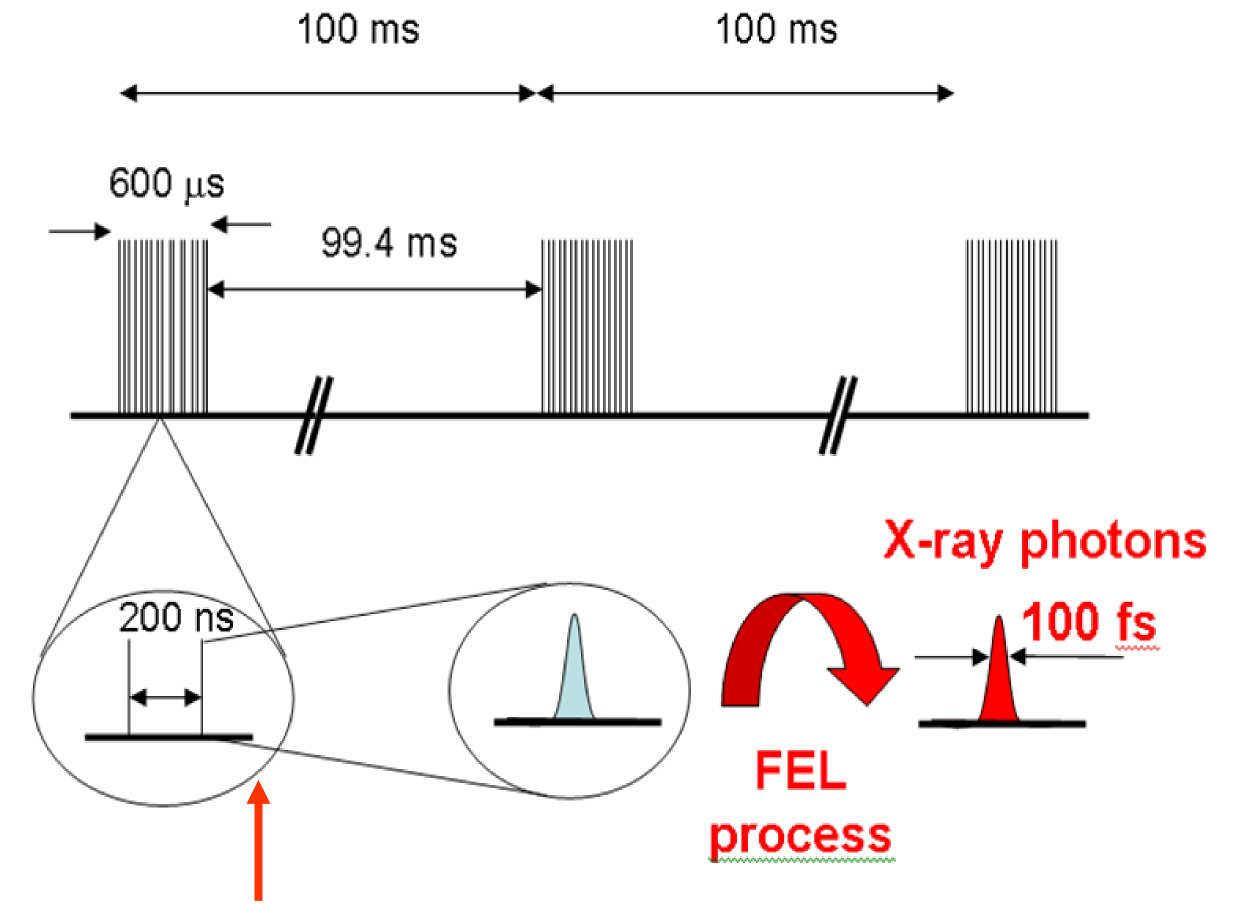


**t > 0.1 s**

**200ns < t < 600 μs:**

**" movie" mode**

**1ps < t< 10 ns:** **"delay-line" mode**

**for "all" times:** **"pump-probe" mode**

# ▪ XPCS at a FEL source: Movie Mode

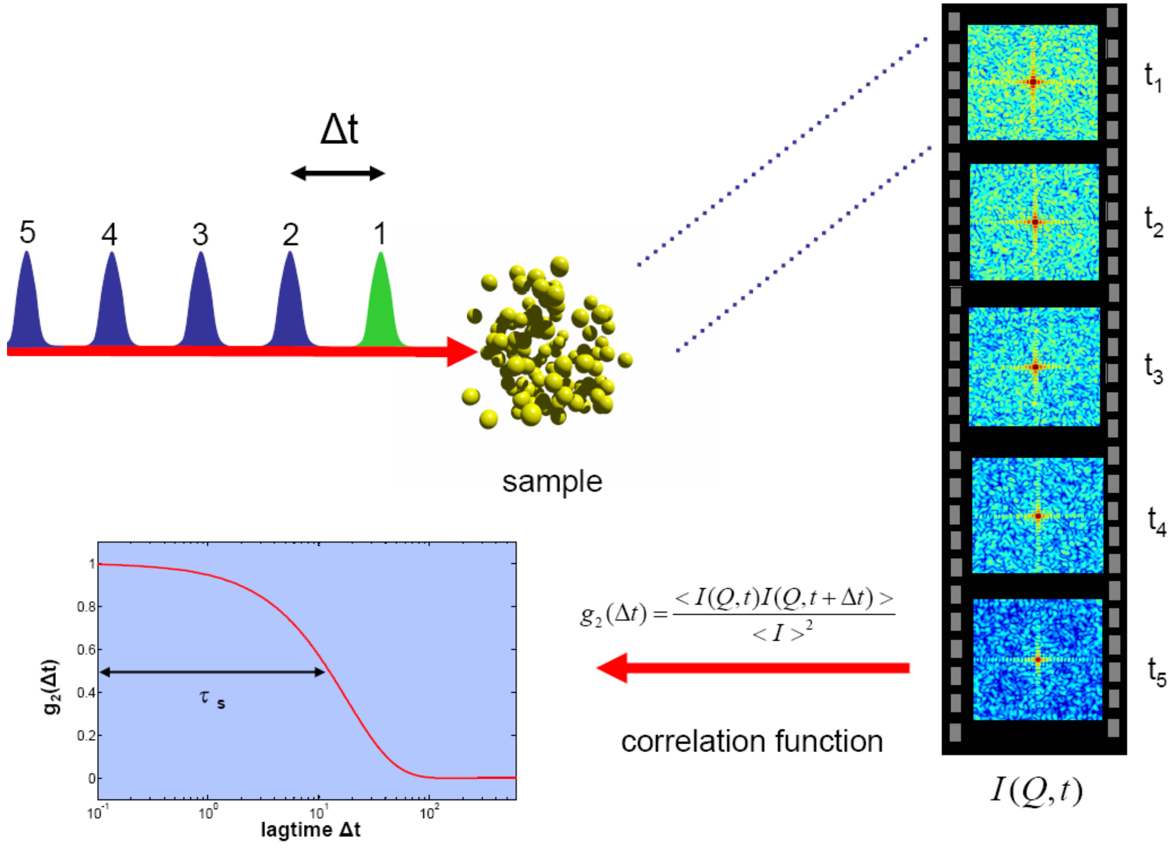

# The Quest for fast 2-D Detectors

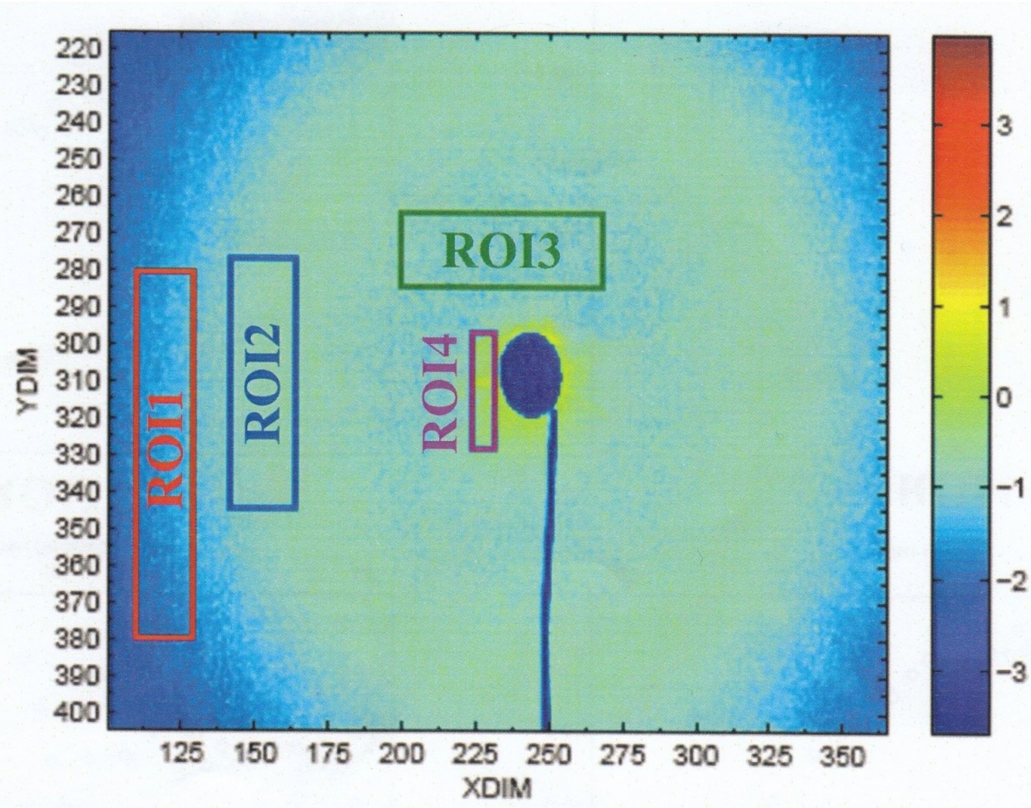


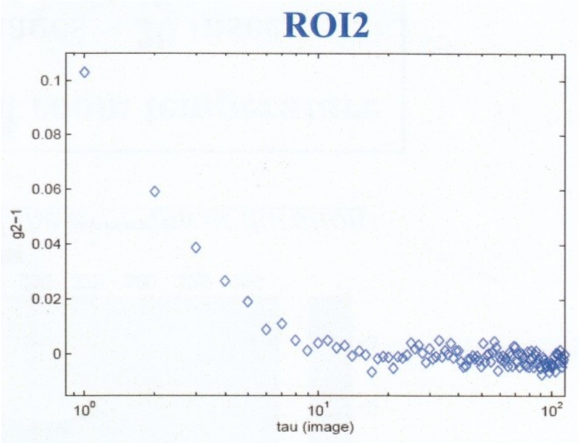


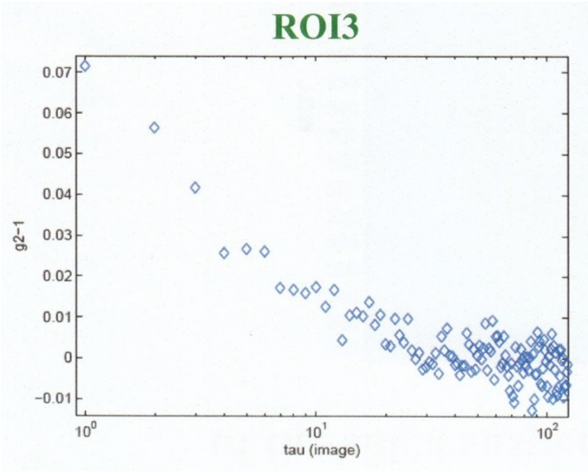


Pilatus detector module: 172 μm pixel size

Silica particles suspended in PPG

sum of 5000 frames with 30 ms exposure

data taken at cSAXS/SLS

# The Quest for fast 2-D Detectors

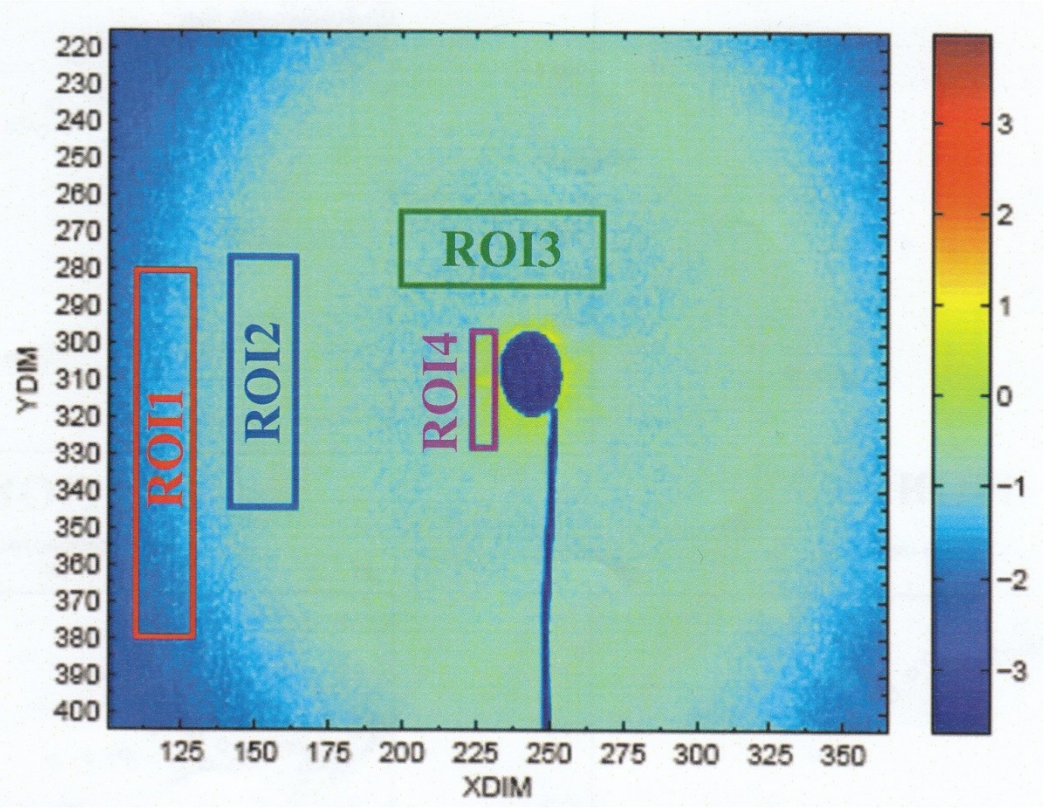


Data acquisition time with 0-D detector: ≈ 2-3 days

Pilatus: sum of 5000 frames with 30 ms exposure separated by a 20 ms delay btw. 2 frames:

Total data aquisition time:
5000x50 ms = 250 s

Estimated data acq. at XFEL:

3000x(100fs+200ns) ≈ 600 μs

# Delay Line Mode

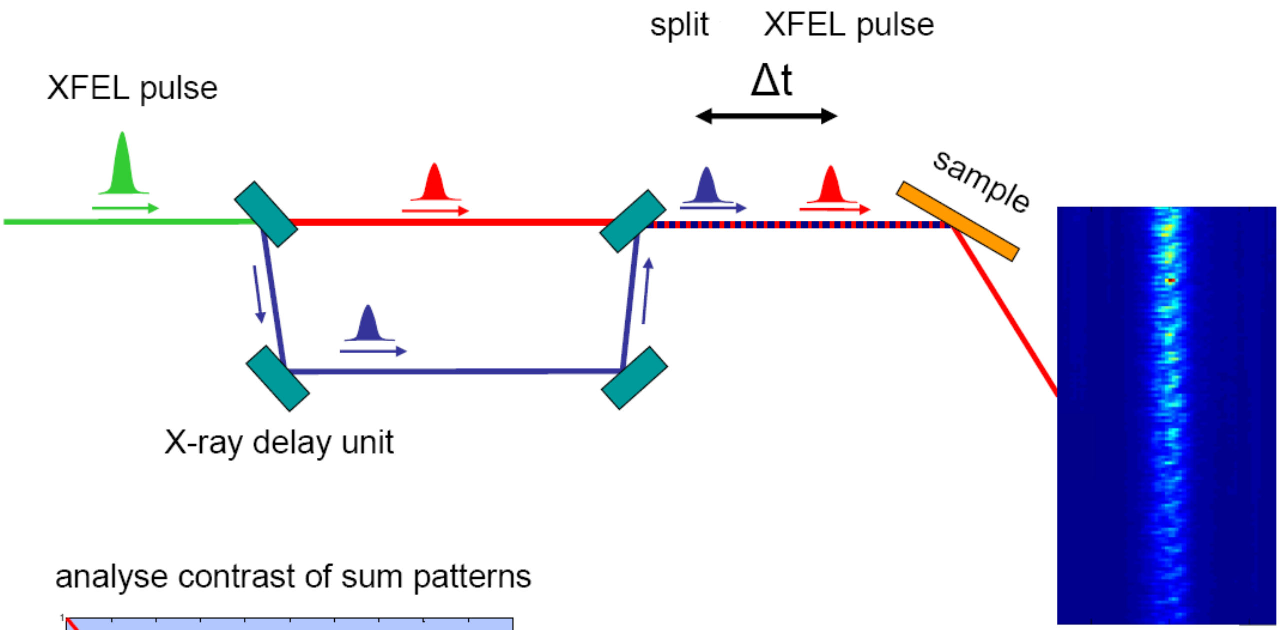


sum of speckle patterns from prompt and delayed pulse recorded on CCD

analyse contrast of sum patterns

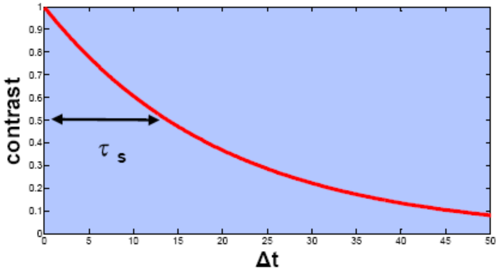


**<u>“Delay Line” Mode:</u>** 1ps < Δt < 10ns (1 ps ⇔ 0.3 mm; 1ns ⇔ 300 mm) “luminosity limited”.

# Delay Line for “hard” X-Rays

**Si(511) at 8.38 keV**

**$\Delta t_{max}$ = 2.8 ns**

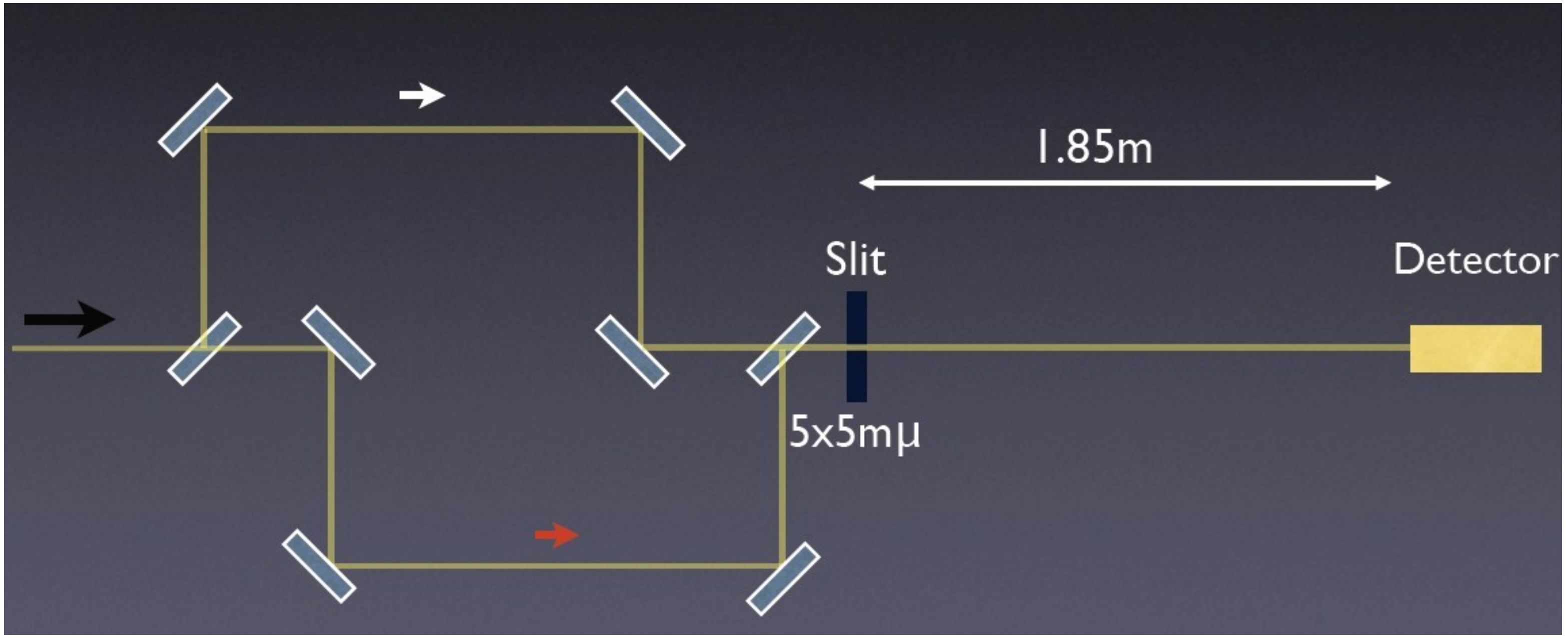


W. Roseker, H. Schulte-Schrepping,
A. Ehnes, H. Franz, O. Leupold and
G. Grübel

# X-Ray delay line

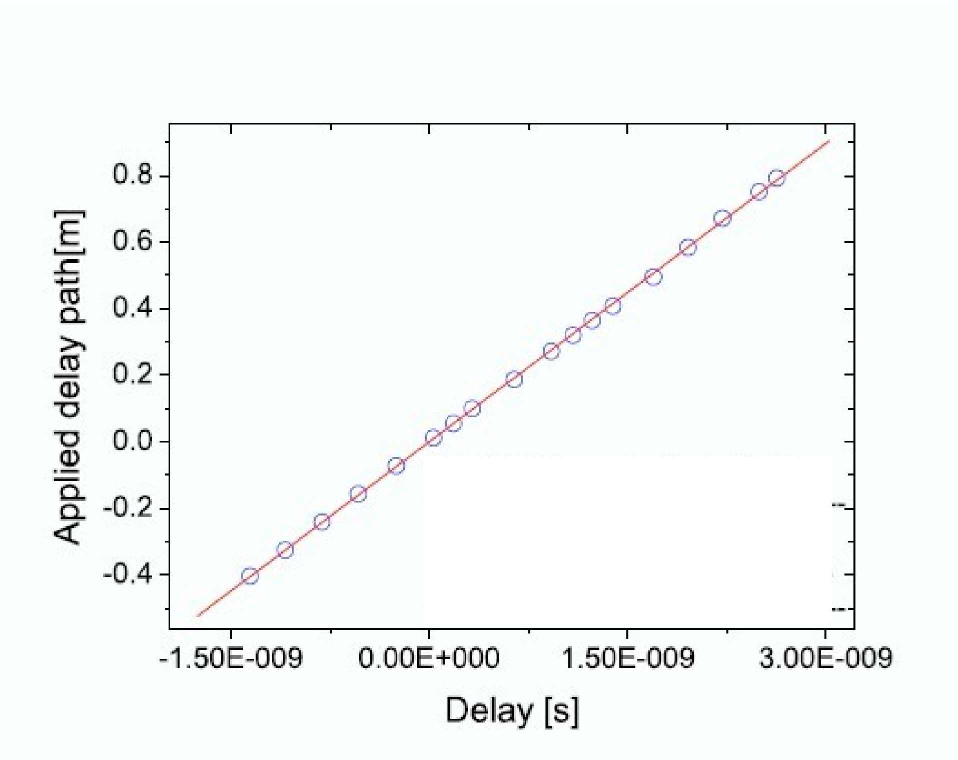


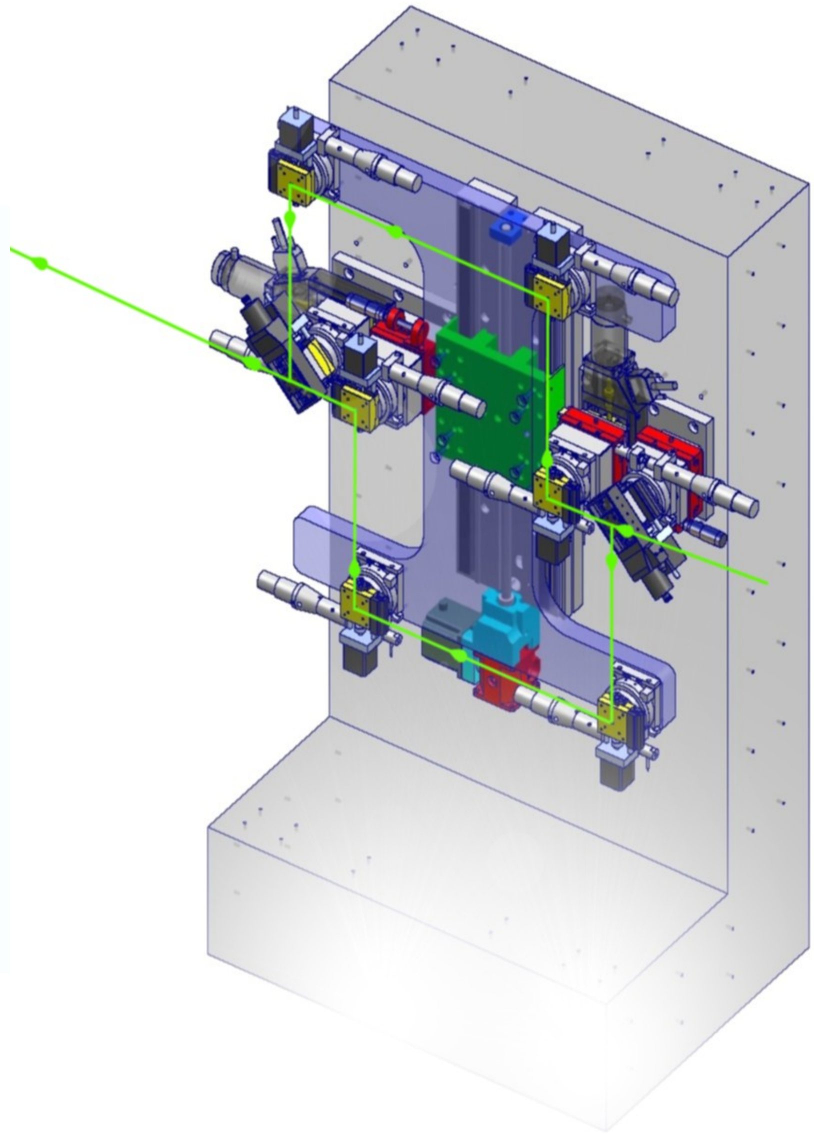

# XPCS at a FEL source: pump-probe mode

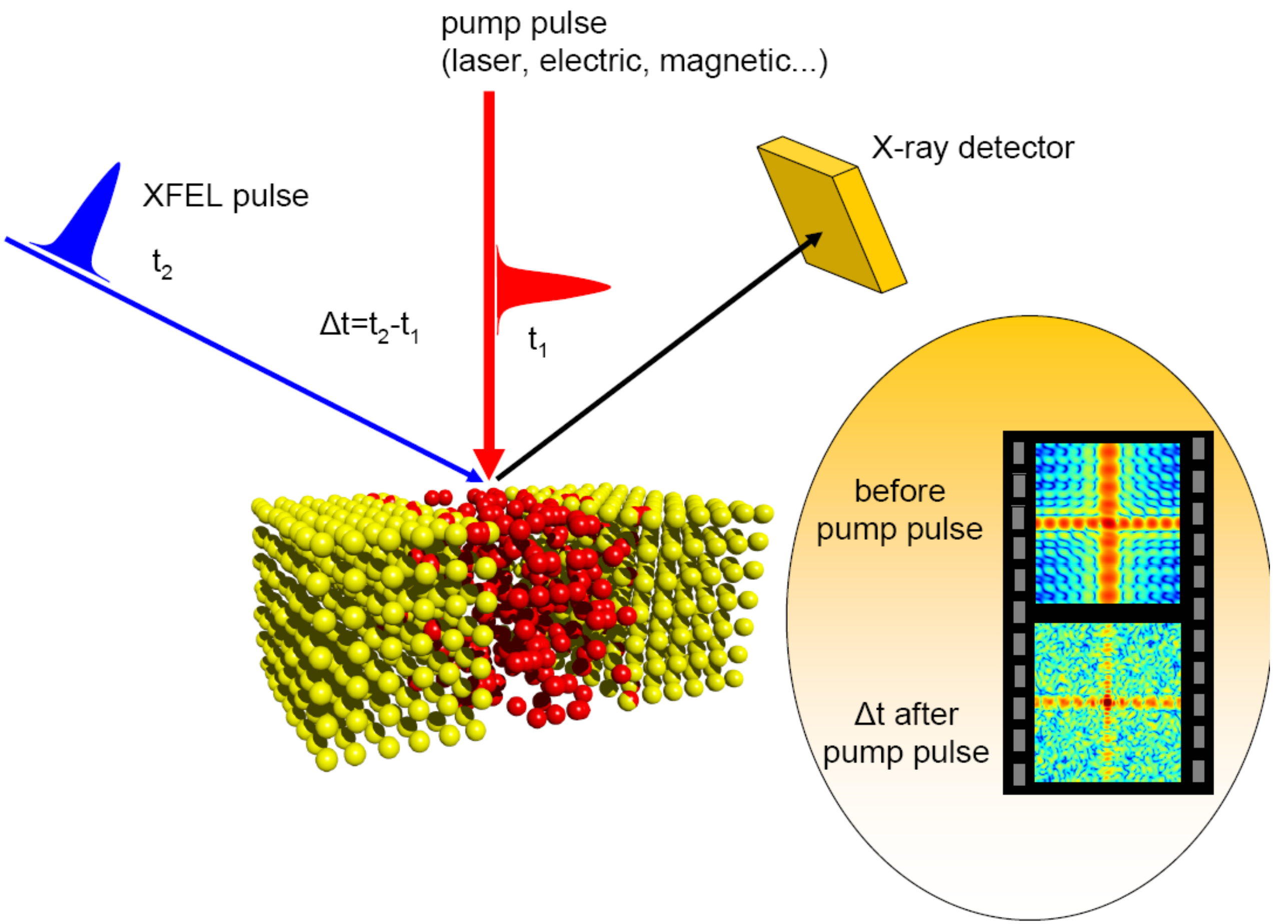

▪

# XPCS at a FEL source

Magnetization Dynamics

Ferroelectrics

Ultrafast dynamics at surfaces and interfaces of liquids

.....

# Ultrafast demagnetization

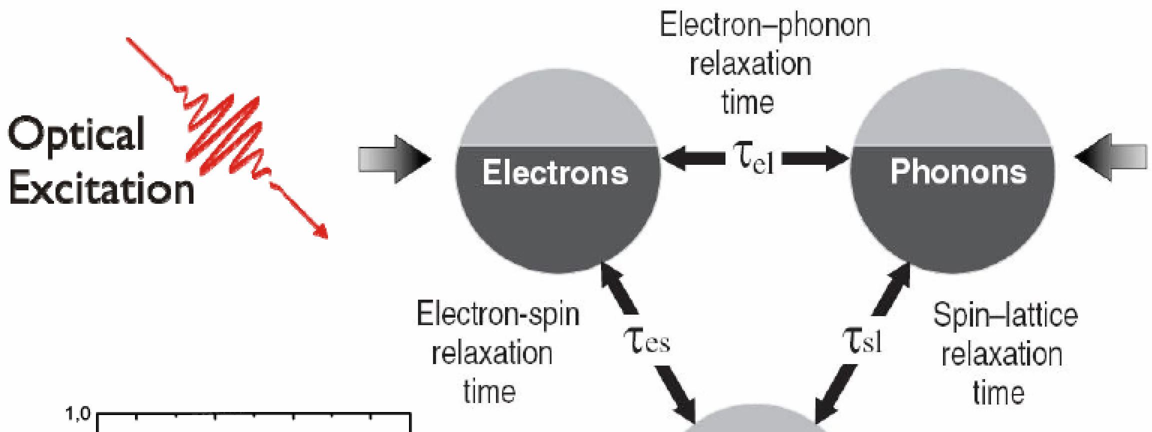


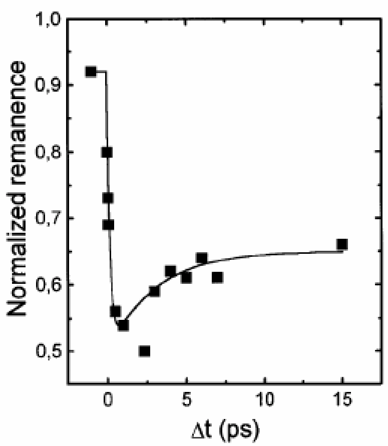


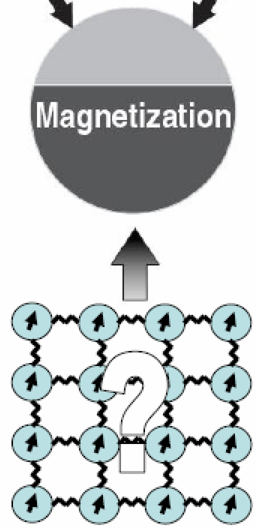


E. Beaurepaire, et al., *PRL* **76**, p4250 (1996)

- spin lattice excitations: domains, vortices spin waves & their non-linear interactions
- optical pump – x ray scattering probe

B. Koopmans et al. Nature Materials 9, 259 (2010)
C. Boeglin et al. Nature 465, 458 (2010)

# Magnetic SAXS data – time dependant

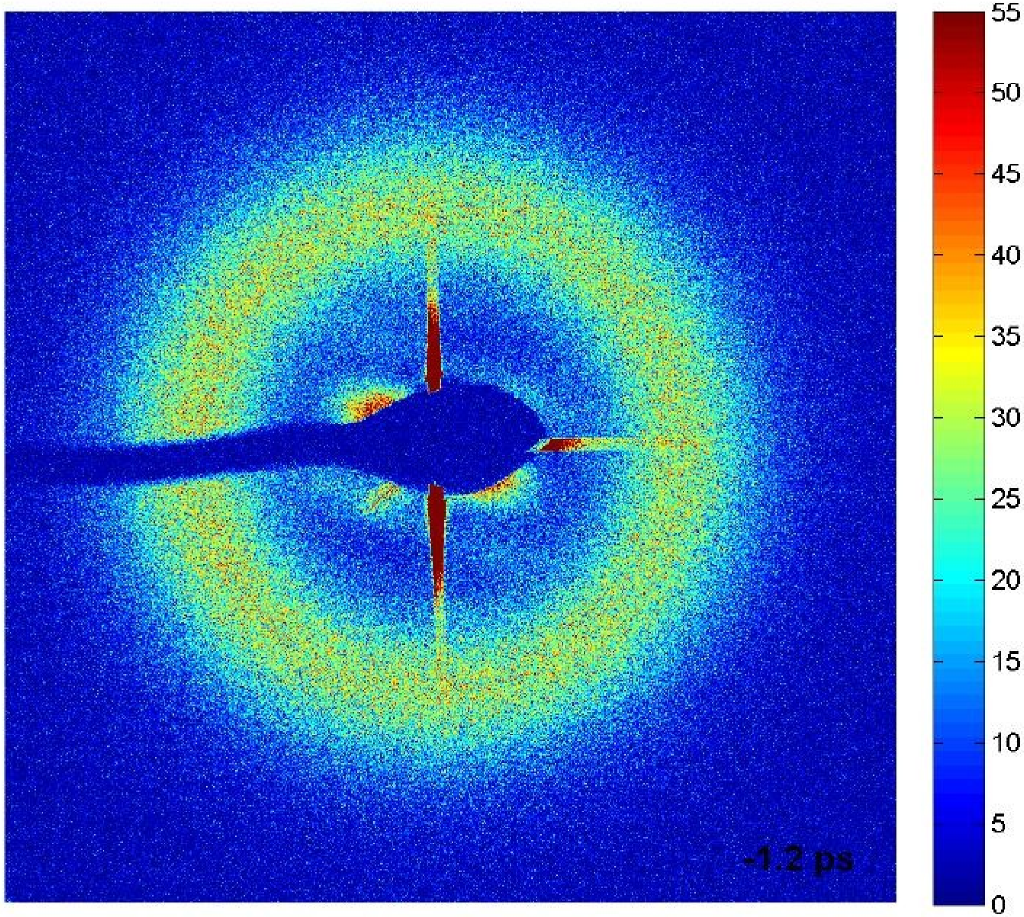


Time-delay scan for 18 $mJ/cm^2$ pumping power, $\Delta t$ = - 1.2 ps...34.5 ps

# Ultra-fast demagnetization from SAXS data

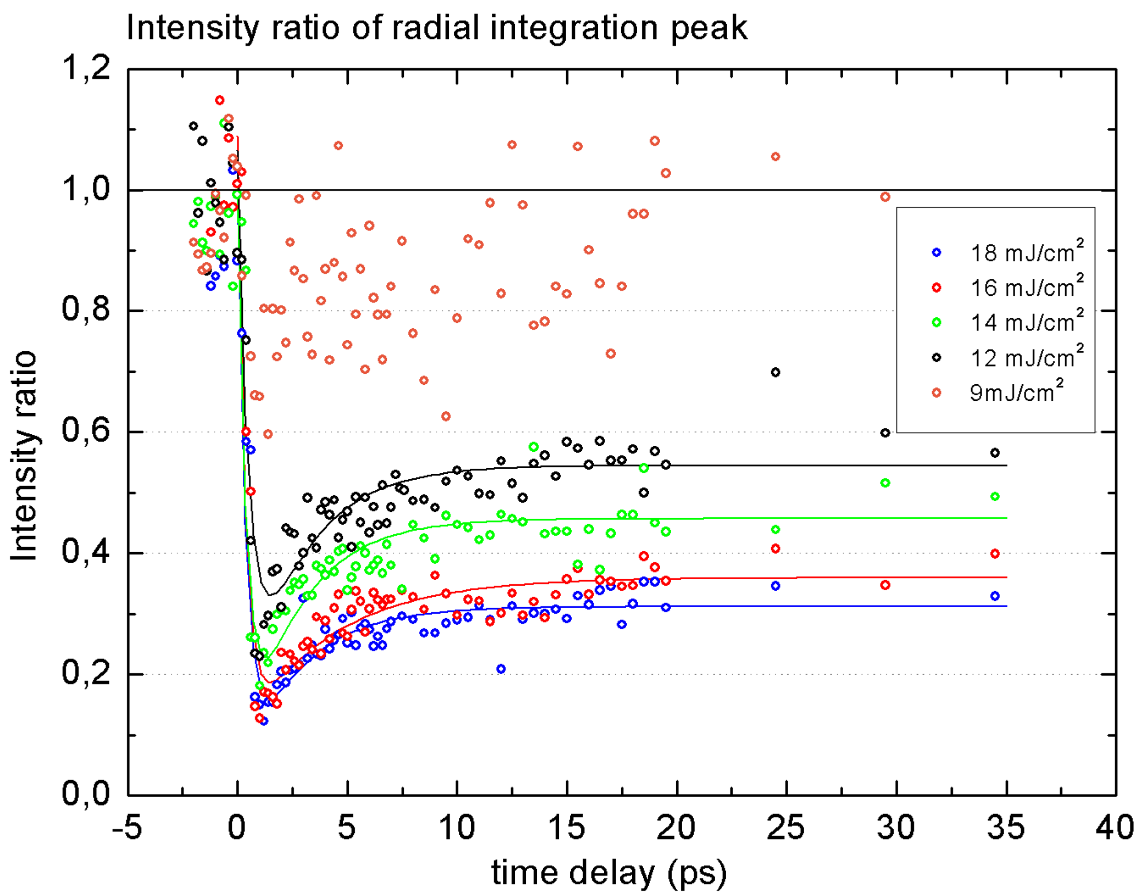


High pump fluence, characteristic demagnetization time below 1 ps

# Polarization Switching in Ferroelectrics

## Domain wall motion during polarization switching in ferroelectric $Pb(Zr,Ti)O_3$

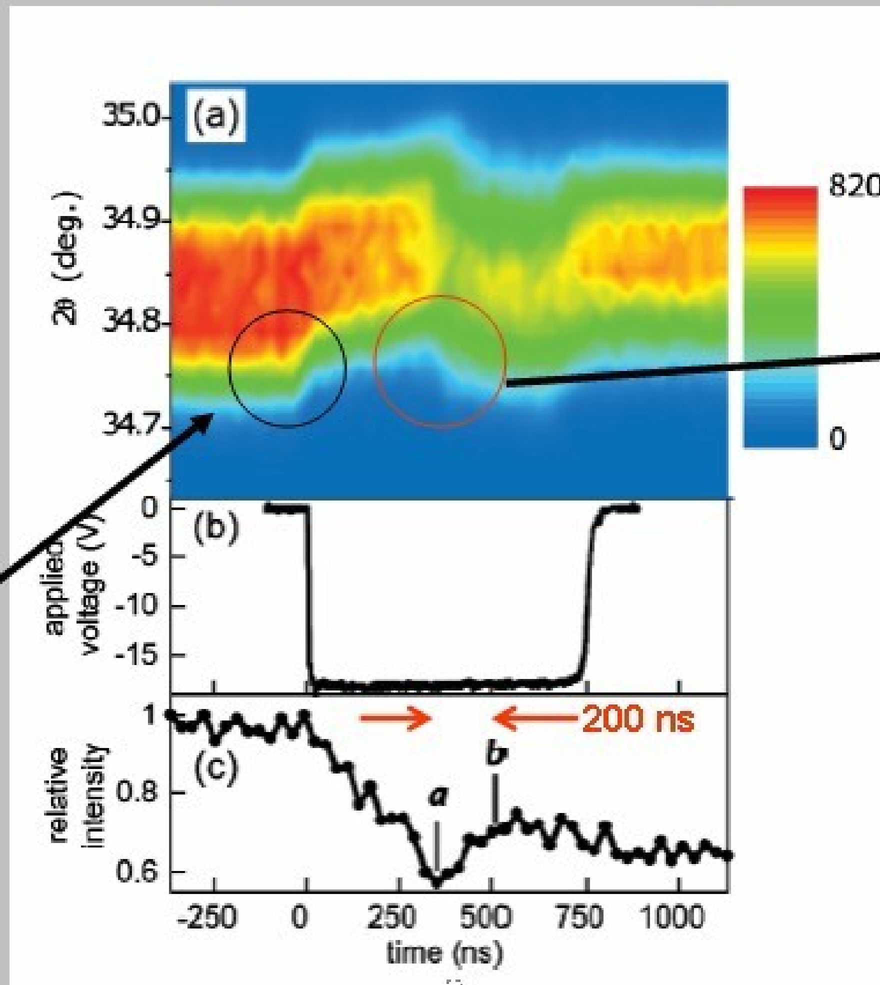


PZT (002) reflection

(0.1 µm, 10 keV, APS)

polarization switching:

Nucleation of domains with reversed polarity, followed by domain growth with domain wall velocities of here about 40m/s.

Study fluctuations and domain growth via XPCS.

lattice shrinkage

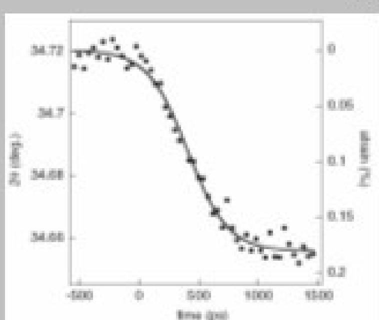

A. Grigoriev, D.-H. Do, D. M. Kim, C.-B. Eom, B. Adams, E.M. Dufresne and P. G. Evans, Phys. Rev. Lett. 96 (2006)187601

# XPCS at a XFEL source: An example

Ultrafast dynamics at surfaces and interfaces in:

- o liquids,
- o membranes,
- o …

**Today:** **$Q_{max} \approx 10^{-4}$ nm$^{-1}$ (water)**

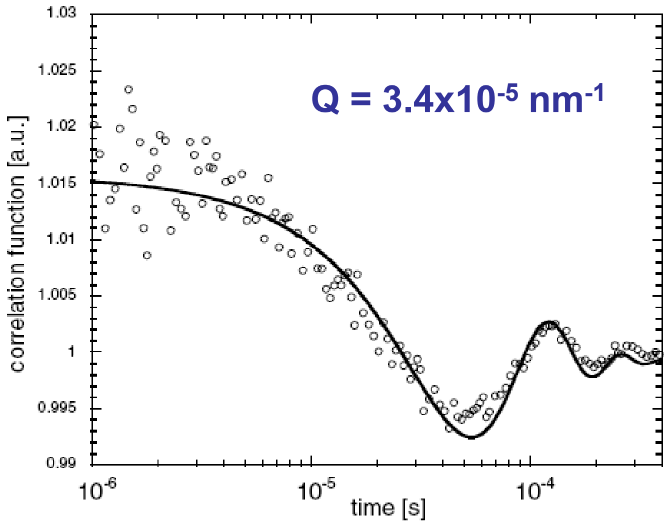


**C. Gutt et al., PRL 91 (2003)76104**

## XFEL:

Onset of non-classical behaviour ($Q > 1$ nm$^{-1}$, beyond continuum hydrodynamics)

Study capillary wave dynamics at high Q in model systems ($\lambda$=1Å, Q=1 nm$^{-1}$)

| | $\tau$ [s] | countrate (FEL) |
|---|---|---|
| **Water** | **≈ 25 ps** | **20** |
| **Mercury** | **≈ 0.5 ps** | **0.3 *** |
| **Glycerol** | **≈ 1 µs** | **3000** |

* expect important deviations due to layering at the surface

**G. Grübel et al., TDR XFEL, DESY (2006)**
**G. Grübel et al., NIM B, submitted**

▪

# The XFEL

www.xfel.eu


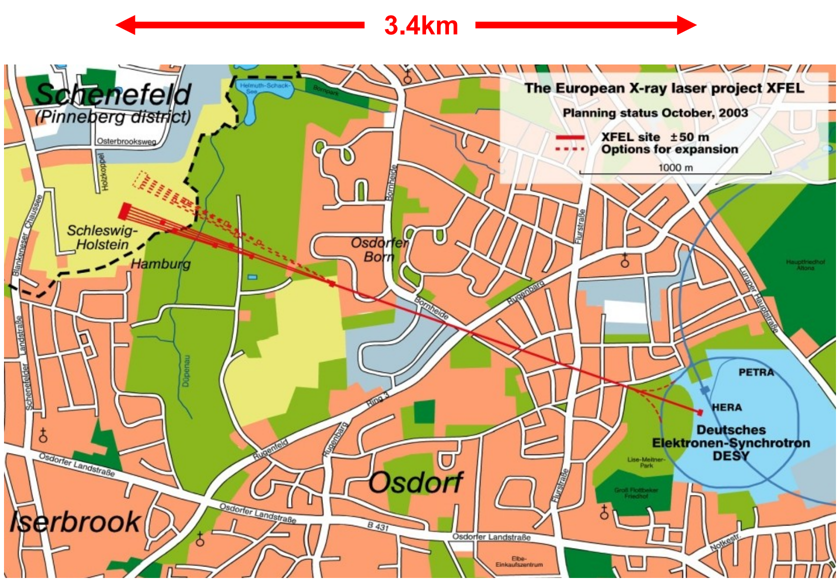


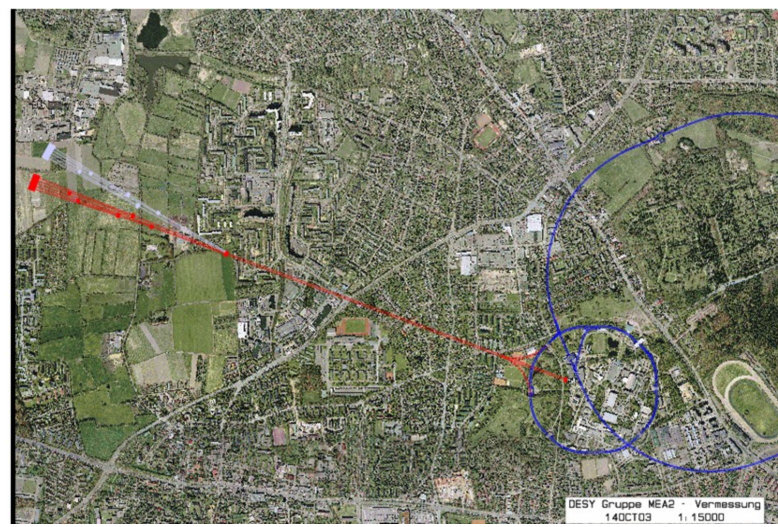

# Acknowledgements

GRK 1355

L. Stadler, C. Gutt, A. Robert